Geoderma 472 (2026) 117904

Contents lists available at ScienceDirect

Geoderma

journal homepage: www.elsevier.com/locate/geoderma

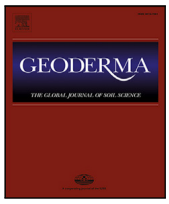

How the landscape influences soil respiration: Explaining spatio-temporal patterns with interpretable machine learning

Maiken Baumberger [a,*], Bettina Haas [b,c], Werner Borken [c], Jakub Nowosad [a,d], Laura Giese [a], Theresa Klein-Raufhake [a], Ute Hamer [a], Nele Meyer [b], Hanna Meyer [a]

[a] Institute of Landscape Ecology, University of Münster, Heisenbergstraße 2, 48149, Münster, Germany
[b] Institute of Physical Geography, University of Frankfurt, Altenhöferallee 1, 60438, Frankfurt am Main, Germany
[c] Institute of Soil Ecology, University of Bayreuth, Dr. Hans-Frisch-Str. 1-3, 95448, Bayreuth, Germany
[d] Institute of Geoecology and Geoinformation, Adam Mickiewicz University, B. Krygowskiego 10, 61-680, Poznań, Poland

ARTICLE INFO

Handling Editor: Jingyi Huang

Dataset link: https://github.com/MaikenBaumberger/SR

Keywords:
Soil respiration
Spatio-temporal
Landscape scale
Random forest
Predictive mapping
Interpretable machine learning
Partial dependency
Shapley additive explanation

ABSTRACT

Soil respiration plays a crucial role in the carbon cycle by representing the greatest flux of carbon from terrestrial ecosystems to the atmosphere. The spatio-temporal variability of soil respiration within a landscape is a result of the patterns of its climatic and environmental drivers. However, despite its importance, the factors driving soil respiration variability within heterogeneous landscapes remain insufficiently understood. To investigate such relationships, we measured soil respiration and determined potential drivers at 166 sites distributed over one year across a 400 km^2 study area in the Fichtelgebirge mountains, Germany. We trained random forest models and applied interpretable machine learning methods to explain and spatio-temporally predict soil respiration. Spatio-temporal patterns of soil respiration were predicted with an RMSE of 61 mg C m^{-2} h^{-1} and an R^2 of 0.39. In the heterogeneous landscape that includes grasslands, arable land, and forests, spatial variability of soil respiration was large, with variations of up to 415 mg C m^{-2} h^{-1} at a single point in time. Spatial patterns of soil respiration followed the patterns of the land use types, were further differentiated by vegetation cover, and were influenced by the topographic position within the landscape. These drivers also influenced patterns of soil temperature, which was the most important driver of soil respiration. Our high-resolution predictions demonstrate pronounced spatial variability in soil respiration at the landscape scale, arising from the interaction of multiple environmental controls, and offer new insights into responses under real-world conditions. Overall, interpretable machine learning showed great potential by explaining the spatio-temporal patterns of soil respiration resulting from complex interactions of its drivers, providing insights into soil respiration on the landscape scale.

1. Introduction

The CO_2 efflux from the soil to the atmosphere (soil respiration), is a key component of the global carbon cycle. It originates from soil organic carbon (SOC) mineralisation (heterotrophic respiration) as well as from roots and root-associated microbes (autotrophic respiration). As a result of increasing temperatures, Bond-Lamberty et al. (2018) reported increased heterotrophic soil respiration rates in recent decades, which goes along with decreasing SOC stocks found by Crowther et al. (2016). However, these trends were observed on a global level, whereas locally these trends can also be fundamentally different. The spatio-temporal variability and the complex interplay of drivers hampers the assessment of the potential responses of this process at different scales (Reichstein and Beer, 2008).

In general, soil properties can be considered at different scales: spatially from pore size to global dimensions and temporally from seconds to millennia. To encompass spatial patterns on the extent of a landscape, a spatial resolution is required in which essential components of the landscape (such as land use type, vegetation cover, terrain and soil properties) can be distinguished (cf. Turner, 1989). In the following we refer to such an extent and resolution by the term "landscape scale". When considering soil respiration in a landscape, significant variations are to be expected, since drivers such as SOC stocks (Haas et al., 2026), soil temperature and soil moisture (Baumberger et al., 2024), as well as physical, physicochemical and biochemical mechanisms (Six et al., 2002; Von Lützow et al., 2008) have high spatio-temporal variability. Therefore, it is of importance to investigate the spatio-temporal patterns of soil respiration at a landscape scale and

* Corresponding author.
E-mail address: maiken.baumberger@uni-muenster.de (M. Baumberger).

https://doi.org/10.1016/j.geoderma.2026.117904
Received 3 June 2025; Received in revised form 15 June 2026; Accepted 16 June 2026

to understand how soil respiration responds to varying environmental conditions. This knowledge is required for predicting dynamics of soil respiration and for developing soil carbon sequestration strategies to mitigate climate change.

Soil respiration is influenced by a multitude of drivers that include soil temperature (Lloyd and Taylor, 1994), soil moisture (Cook and Orchard, 2008), soil organic matter quantity and composition (Cleveland et al., 2007), nutrient availability (Meyer et al., 2018b), and vegetation density and vitality (Raich and Tufekcioglu, 2000), among other factors. Soil temperature and soil moisture regulate microbial activity, which generally increases with temperature up to about 35°C (Richardson et al., 2012) but declines under extreme moisture conditions due to limited water or oxygen availability (Moyano et al., 2012). Nutrients and carbon availability influence the growth and activity of microorganisms, whereby a high C/N ratio may indicate nitrogen limitation, possibly reducing microbial growth and microbial activity (Meyer et al., 2018b). Local soil properties such as pH influence the composition and activity of microbial communities. The activity of microorganisms is crucial for the mineralisation of SOC and therefore for the amount of CO_2 released through heterotrophic soil respiration. The autotrophic component of soil respiration is strongly dependent on vegetation characteristics such as plant activity and root biomass (Shibistova et al., 2002). Since soil respiration is influenced by a multitude of external environmental factors, it exhibits spatial and temporal variations across a landscape.

Temporal variations in soil respiration are the result of variations in meteorological conditions. Borken et al. (2002) and Tang and Baldocchi (2005) have shown for different ecosystems that soil respiration follows the temporal variations of soil temperature, resulting in annual, interannual and diurnal variations of soil respiration. Periods of drought reduce soil respiration and wetting of dry soil may lead to short-term increases in soil respiration (Borken and Matzner, 2009). The vegetation phenology also leads to temporal changes in soil respiration. Besides plant activity, vegetation influences soil respiration through the amount and composition of litter and roots (Liu et al., 2023; Bardgett et al., 2014).

The interplay between meteorological conditions and landscape characteristics drives spatial variability of soil respiration. More precisely, local weather conditions, buffered by the vegetation cover and influenced by the terrain as well as structural soil properties, result in fine-scale spatial variations of soil temperature and soil moisture (Baumberger et al., 2024), which strongly influence spatial patterns of soil respiration (Reichstein et al., 2003). Martin and Bolstad (2009) have analysed the spatial variations of soil respiration along different spatial scales and detected major variations at a scale of 100 m, which were primarily driven by spatial variations of soil temperature and soil moisture. Meyer et al. (2018a), furthermore, have shown spatial differences in heterotrophic soil respiration depending on land use. Under similar soil temperature and soil moisture conditions, the CO_2 efflux of forest soils was highest, followed by grasslands and arable land. Soil properties differ between land use types, but also within each land use type, which further contributes to the development of spatial patterns of soil respiration. For instance, positive effects of pH, SOC, and total nitrogen content on soil respiration were observed by Borken et al. (2002) for forest sites.

Furthermore, it needs consideration that the CO_2 efflux at the soil surface is a product of the entire soil profile (Hirano, 2005). Therefore, not only the state of drivers at the soil surface is important, but also the soil properties at deeper depths need to be considered. Hence, soil respiration on the landscape scale is shaped by a complex interplay of numerous vertically, spatially, and temporally varying drivers, resulting in fine-scale patterns along all dimensions.

This complexity makes data collection challenging, leading many studies to either focus on temporal or spatial variations. Soil respiration measurements are typically only snapshots in a changing environment, since measurements often last only a few minutes. Depending on the research question and due to the associated costs and effort, there is a trade-off between conducting many temporal replicates on a few sites (e.g., Borken et al., 2002; Subke et al., 2003) and conducting few or no temporal replicates on many sites (e.g., Crum et al., 2016). When focussing on temporal variability and experimental manipulations, mainly single ecosystems (e.g., one forest type) are considered (e.g., Schindlbacher et al., 2015). Studies that analyse the spatial variability of soil respiration are also often based on measurements from a single agricultural field (e.g., Borchard et al., 2015; Prolingheuer et al., 2014). There are only a few studies investigating the spatio-temporal variability of soil respiration on a landscape scale. Here, the landscape in Martin and Bolstad (2009), Euskirchen et al. (2003), or Shi and Jin (2016) was limited to forest ecosystems. Crum et al. (2016) investigated a more heterogeneous landscape that includes lawns, agriculture, and wild land. Further studies focussing on soil respiration in a heterogeneous landscape are investigations of the temperature dependency of soil respiration (Q10) influenced by different site conditions (e.g., Meyer et al., 2018a; Chatterjee and Jenerette, 2011), but these studies are in most cases based on laboratory experiments and do not consider the actual environmental conditions. Although it is of great interest to realistically quantify the CO_2 efflux on a landscape scale, comprehensive studies on spatio-temporal soil respiration variability in heterogeneous landscapes under natural conditions, accounting for multiple drivers, remain scarce.

By spatio-temporal modelling of soil respiration measurements, insights into the spatio-temporal patterns of soil respiration could be provided. In models, the potential drivers of soil respiration are described by predictors, which can be either direct measurements of drivers such as soil temperature or proxies of drivers such as indices from satellite images like the Normalised Difference Vegetation Index (NDVI) for vegetation vitality. To account for the complexity of predictors and their interactions, machine learning algorithms are promising modelling tools. Due to their large number of trainable parameters which are fitted in the modelling process, these models are capable of capturing complex relationships in data and achieving high predictive performance. However, this also requires a large number of data points as training data from which these relationships can be learned. Although the relationships learned by the model reflect patterns in the data rather than causal relationships (Wadoux et al., 2020), they can serve as a baseline to interpret patterns and generate new hypotheses. Random forest models (Breiman, 2001), in particular, are often used to model and explain relationships in data with a large number of predictors. They have been applied frequently in spatio-temporal modelling (Lary et al., 2016) and were proven to be an effective tool for spatio-temporal prediction tasks (Gasch et al., 2015; Baumberger et al., 2024). With the increasing development of interpretable machine learning methods, it is becoming increasingly feasible to gain insights into the learned relationships, eventually allowing to support an understanding of the underlying processes (Jiang et al., 2024). For instance, partial dependency enables to show the mean relationship of each predictor to the target variable (Friedman, 2001). Interpretation techniques such as Shapley additive explanation (SHAP), can show the marginal effects of individual predictors (Lundberg and Lee, 2017). Applying Shapley additive explanation to spatial continuous predictor data allows to determine the contribution of each predictor for each location in a study area. This method has already been used by, e.g., Wadoux et al. (2023), to analyse the regional drivers of SOC stocks across France.

In this study, we aim at investigating spatial and temporal variations of soil respiration on a landscape scale. Therefore, we selected a 20 km × 20 km study area in the Fichtelgebirge Mountains, Germany. The selected landscape is characterised by forests, grasslands, and arable lands and is located in a low mountain range, resulting in an elevation difference of 566 m across the area. Within this landscape, we conducted measurements of soil respiration and its drivers (including soil temperature, soil moisture, SOC stocks, C/N ratio, pH, bulk density, and water holding capacity) at 166 locations distributed over one

year. The measurements were complemented with data describing the landscape characteristics such as land use type, slope, topographic wetness index, vegetation vitality, and vegetation change. Using this dataset, we aim to analyse the influence of the drivers shaping the spatio-temporal patterns of soil respiration across a landscape. For this purpose, we (1) develop a model to predict and explain soil respiration. By predicting soil respiration with a target resolution of 10 m and 1 h for the study area, we (2) investigate the variability of soil respiration in a heterogeneous landscape. Since there is still little knowledge about the drivers of the spatio-temporal patterns of soil respiration on the landscape scale, we (3) determine the most important predictors of soil respiration and analyse the contribution of all predictors on soil respiration within the study area by applying interpretable machine learning methods.

2. Methods

2.1. Study area

The study area covers 400 km^2 of a low mountain range landscape, the Fichtelgebirge mountains in Germany (Fig. 1). The extent of the squared area is defined by the coordinates: 11.72°E – 11.99°E, 50.05°N – 50.24°N. A granite mountain range stretches diagonally from south-west to north-east through the study area, having its highest point at an elevation of 1034 m a.s.l.. While the mountain range is used for forest cultivation, the lower plains with the lowest point at 468 m a.s.l. are characterised by a mixture of arable land and grasslands including small forest patches. A large part of the study area is covered by terrestrial soils such as Cambisols and Cambic Podzols. There are also semi-terrestrial and stagnic soils such as Gleysols and Stagnosols (FAO; Bayerisches Landesamt für Umwelt, 2020). The main soil texture in the study area is loam (FAO). The spatial distribution of land use type, aggregated soil group, and elevation within the study area is shown in Baumberger et al. (2024). The study area has a temperate climate with a mean annual temperature of 6.5°C and an annual precipitation sum of 1064 mm, measured in the centre of the study area for the period from 2001 to 2010 (Foken, 2017).

2.2. Soil respiration measurements

2.2.1. Sampling design

To capture soil respiration on a landscape scale, we measured soil respiration on grasslands, arable land, and forests throughout the study area. From December 2021 to December 2022, we conducted 191 soil respiration measurements at different times of a day and across the different seasons of the year and thus under a variety of weather conditions (Figs. 1 and 4). Repeated measurements were taken at nine sites (one in each season), while all other sites were measured only once, resulting in a total of 166 different measurement sites. The measurements were divided approximately equally between the 3 different land use types in the study area: forest (n = 64), grassland (n = 53), and arable land (n = 74). For the selection of a measurement site, it was essential that the surrounding area exhibited sufficient homogeneity to ensure that the site represented the characteristics of a 10 m × 10 m satellite pixel (see Section 2.3). The spatio-temporal soil respiration measurements were part of a more extensive measurement campaign, the Carbon4D project, founded by the German Research Foundation (project number 455085607). Due to different objectives in the project, the measurements followed two different sampling designs (indicated in Fig. 1 by different coloured dots):

- **Sampling design "SR + SP + SC":** 91 measurement sites were selected by the sampling design "SR + SP + SC" (cf. Fig. 1), where the abbreviations refer to: SR = soil respiration measurement, SP = soil probes for soil temperature and soil moisture measurement, and SC = extraction of soil cores. In this sampling campaign, we subdivided the square study area into an 8 × 8 grid and randomly selected a grid cell. Within the grid cell, we selected a location of a previously defined land use type (forest, grassland, or arable land) based on accessibility and permission to access. Only terrestrial soils were considered in this sampling design (i.e., soils with fluvial or groundwater influence were excluded). Almost every week, one random plot within each of all three land use types was selected. We further chose three fixed measurement sites per land use to obtain temporal replicates by measuring soil respiration and predictors in each season of the year at the same location.
- **Sampling design "SR + SP":** The data were complemented with 75 measurements from a second parallel running sampling design. Here, only soil respiration measurements (SR) and soil temperature and soil moisture measurements with soil probes (SP) were conducted. To take samples following the sampling design "SR + SP" (cf. Fig. 1), we categorised environmental soil classes for stratification. Environmental soil classes describe the landscape through a combination of land use, aggregated soil group, and soil texture (cf. N. Meyer et al., 2018; Baumberger et al., 2024). By taking a stratified random sample across the environmental soil classes, we endeavoured that the selected measurement sites represent the distribution of land use and soil properties in the study area.
- **Sampling design "SR":** In addition to the spatio-temporally distributed soil respiration measurements, we also used a data set of soil respiration measurements (SR; Muhr and Borken, 2009) that contained measurements from one single location at different points in time (sampling design "SR" in Fig. 1). 60 measurements were taken between 2007 and 2011 in the centre of our study area (coordinates: 50.14°N, 11.87°E). The site is located at an elevation of 770 m a.s.l. in a coniferous forest dominated by the species *Picea abies*. The soil is classified as Haplic Podzol with a sandy loam texture (Schulze et al., 2009). As the soil respiration measurements were conducted at one site, differences in measurements were therefore not influenced by changing site-specific characteristics but only by seasons and weather conditions.

2.2.2. Closed chamber measurements

We measured soil respiration with portable closed chamber measurements, using the same methods and instrumentation that were previously used in several studies such as Muhr and Borken (2009) and Muhr et al. (2009). Using this method, the CO_2 efflux at the soil surface is captured, which is composed of heterotrophic respiration and autotrophic respiration. For closed chamber measurements, the following procedure was implemented at each of the 166 measurement sites: A PVC collar was pushed into the soil until it was firmly sealed. The PVC collar had an inner diameter of 0.47 m with a corresponding volume of 0.037 ± 0.007 m^3 (varying volumes due to different installation heights). We removed above-ground biomass to avoid an influence of the plants during the measurement. The installation of the PVC collar and the biomass removal was done 30 min before the actual measurement. In previous experiments, we showed that there is no significant difference when placing the chamber 24 h as compared to 30 min before the measurement, indicating that 30 min after the placement of the PVC collar no installation-related effects occur. To start the soil respiration measurement, a PVC lid connected to a portable Infrared Gas Analyser (LI-820, LI-COR, Nebraska, USA) was placed onto the collar. To ensures the mixing of air, a waiting period of 30 s was applied before the measurement was initiated. The air circulated with a flow rate of 0.5 l/min between the chamber and the Infrared Gas Analyser, while a logger recorded the increasing CO_2 concentration every 10 s for 5 min. We repeated the CO_2 measurements 3 times at the same location. Between each measurement, the lid was removed for at least two minutes. In addition, we measured head space temperature, soil temperature in the top 10 cm of the soil, and atmospheric pressure.

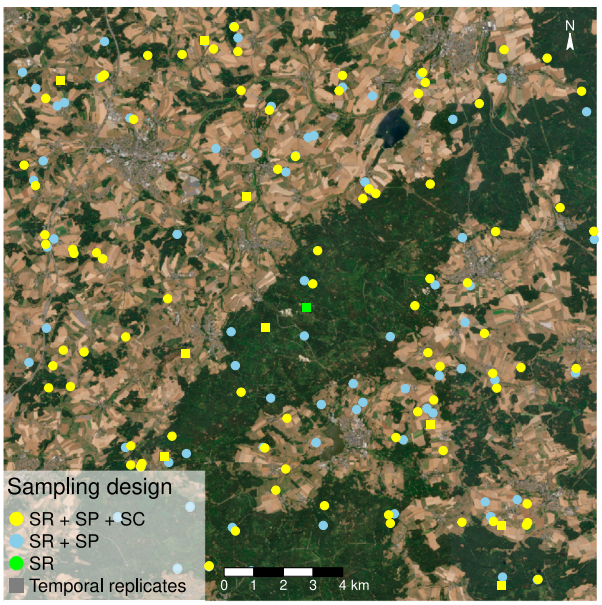

Fig. 1. Measurement sites in the study area (coordinates: 11.72°E – 11.99°E, 50.05°N – 50.24°N) indicated on the RGB Sentinel-2 image from the 25th July 2022. Soil respiration was measured following three different sampling designs, indicated by different colours. Explanation of abbreviations: SR = soil respiration measurements, SP = soil probe measurement for soil temperature and soil moisture, SC = extraction of soil cores. Squares indicate measurement sites with temporal replicates (up to 4 for the yellow dots and 60 for the green dot).

The soil CO_2 efflux in mg C m^{-2} h^{-1} was calculated with a linear regression of the CO_2 concentration over time ($\Delta c/\Delta t$), using the molecular weight of carbon (M_i), the chamber volume (V), the soil surface area (A), the head space temperature (T) and the atmospheric pressure (P):

$$CO_2\ \text{efflux} = \frac{\Delta c}{\Delta t} \cdot \frac{V}{A} \cdot \frac{P}{(8.314 \cdot T)} \cdot M_i \quad (1)$$

For further analysis, only measurements with an $R^2 > 0.5$ were considered and the mean CO_2 efflux of the replicates was calculated.

2.3. Predictor variables

Predictor variables were used to explain and model soil respiration on the landscape scale. For spatial modelling, the predictor variables had to be available as raster data. We aimed at using a spatial resolution of 10 m in order to capture important structures in the landscape. When combining the chamber measurements with all predictor data, we used the Sentinel-2 satellite grid as a basis and extracted the values of the predictor variables of the corresponding 10 m × 10 m pixels. Likewise, each soil respiration measurement represented one entire pixel by selecting a representative measurement point. If the predictors were used exclusively to explain relationships, point measurements were sufficient. The predictor data in this study consisted of (1) point measurements associated with the soil respiration measurements (Section 2.3.1), (2) raster products modelled from these point measurements (Section 2.3.2) and (3) generally available raster products such as soil maps and satellite images (Section 2.3.3).

2.3.1. Measurements of predictor variables

At all measurement sites, except the long-term soil respiration measurement in the centre of our study area, we measured depth-resolved soil temperature and volumetric soil moisture with soil probes (Drill & Drop Probe RS232, Sentek Technologies, Australia). The soil probes have a length of 90 cm and measure soil temperature and soil moisture in 10 cm segments. Additional information on these measurements can be found in Baumberger et al. (2024). For all of the measurement sites in the "SR + SP + SC" sampling approach, we additionally took 1 m deep soil cores with 8 cm diameter. We extracted them with a percussion drill (Cobra, Atlas Copco, Sweden) within a maximum distance of 3 m to the chamber. We divided these cores into 10 cm segments and further analysed them in the laboratory. We determined the water holding capacity (WHC), gravimetric water content, pH(H_2O), bulk density as well as carbon and nitrogen content of the samples. We calculated the C/N ratio, as well as the SOC stocks, based on the measured carbon content, nitrogen content, and bulk density (Haas et al., 2026). We used the gravimetric water content and the WHC to estimate the percentage of water holding capacity reached in each sample at the time of sampling (in the following referred to as % WHC).

As soil respiration represents the sum of CO_2 released from all depths and transported upward to the surface, the soil conditions in deeper soil layers may also have an influence on soil respiration. Therefore, we included soil temperature, soil moisture, and SOC stocks from different depths. We aggregated the depth-resolved soil temperature, soil moisture, and SOC stocks into soil surface (0–10 cm for grasslands and arable land; organic layer in forests) and lower topsoil (10–30 cm for grasslands and arable land; 0–30 cm in forests). In forests, the organic layer in most cases had a thickness of 10 cm. Soil temperatures and soil moisture were averaged vertically, and SOC stocks were summed vertically. For C/N ratio, bulk density, % WHC, and pH we used the measurements from the upper 10 cm of the soil.

2.3.2. Spatially interpolated predictor variables

For spatial prediction of soil respiration, the availability of spatially continuous predictor data is required (cf. Fig. 2 and Table 1). Soil temperature, soil moisture, and SOC stocks are three of the most important predictors (Curiel Yuste et al., 2007). As part of the Carbon4D research project, machine learning models for spatial predictions of soil temperature, soil moisture, and SOC stocks were developed based on their point measurements (described in Section 2.3.1; Baumberger et al., 2024; Haas et al., 2026). The models predict soil temperature and soil moisture for the entire study area with a spatial resolution of 10 m and a temporal resolution of 1 h, as well as SOC stocks with a spatial resolution of 10 m. The model performance evaluation showed an RMSE of 1.22°C and an R^2 of 0.95 for soil temperature predictions, an RMSE of 5.98% and an R^2 of 0.47 for soil moisture predictions, and an RMSE of 7.61 t/ha and an R^2 of 0.78 for predictions of SOC stocks (Baumberger et al., 2024; Haas et al., 2026).

Even though the models for soil respiration in this study (see Section 2.5.1) were trained directly with measurement data of soil temperature, soil moisture, and SOC stocks, data gaps in the measurement data were filled by the respective machine learning model. For SOC stocks, measurement data only existed where soil cores were taken, and soil temperature and soil moisture contain some data gaps due to incomplete installation of the soil probes. For the 166 measurement sites, 5%–25% of the soil temperature and soil moisture data needed to be modelled depending on the depths and for the SOC stocks 40% of the data were missing and needed to be filled.

2.3.3. Spatially available predictor variables

We further used land use types, topographic information, and satellite images as spatially continuous predictor variables. The land use type was determined based on a map of the actual use (Bayerische Vermessungsverwaltung, 2020c) and the soil estimation (Bayerische Vermessungsverwaltung, 2020a), which we used to separate arable land and grasslands. We used further predictors describing the relief of the landscape, by processing the digital elevation model (Bayerische Vermessungsverwaltung, 2020b). The slope was calculated from the elevation differences in the digital elevation model. Based on the digital elevation model, information on relief-related run-off and soil moisture can be described by the topographic wetness index (TWI). The TWI was

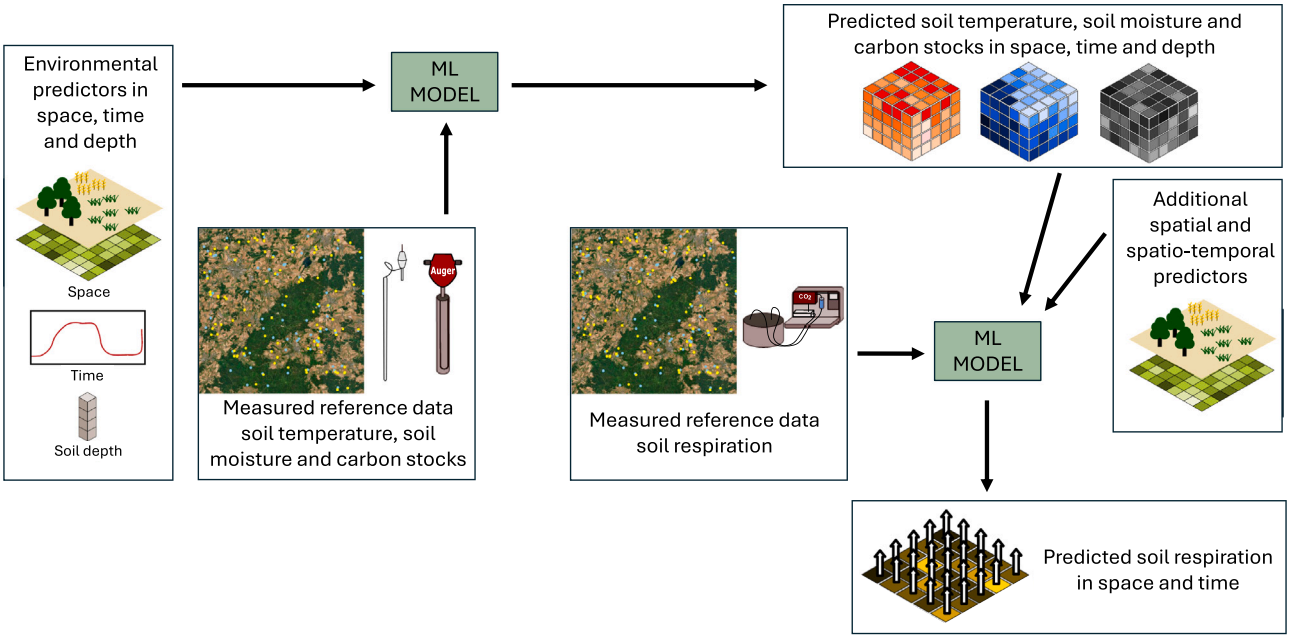

Fig. 2. Sketch of the workflow of the spatial prediction of soil respiration. Measured reference data of soil temperature, soil moisture and SOC stocks were each combined with their predictor variables in a machine learning model. The models were used to predict soil temperature, soil moisture and SOC stocks in space, depth and time (details described in Baumberger et al., 2024 and Haas et al., 2026). Reference data of soil respiration and its predictor variables were used in a subsequent machine learning model to learn the relationships. Here, conditions of deeper soil depths were also considered, as soil respiration at the surface is product of the entire soil profile. The soil respiration model was applied to the spatial raster data of the predictor variables, including the spatial predictions of soil temperature, soil moisture and SOC stocks, to predict soil respiration in space and time.

Table 1
Predictor variables of soil respiration used in this study. The differentiation between point data and raster data indicates whether the respective variable was available at the measurement sites only or spatially continuos in the study area. In the point data column, indicates x in-situ and laboratory measurements and (x) extracted values from raster products. In the raster data column, indicates x the raster products and (x) spatially modelled raster data sets. The source of the data products is also given. Explanation of abbreviations: SOC = soil organic carbon, % WHC = percent of water holding capacity, TWI = topographic wetness index, NDVI = Normalised Difference Vegetation Index.

Predictor	Point data	Raster data	Source of raster data
Soil temperature (0–10 cm)	x	(x)	Baumberger et al. (2024)
Soil temperature (10–30 cm)	x	(x)	Baumberger et al. (2024)
Soil moisture (0–10 cm)	x	(x)	Baumberger et al. (2024)
Soil moisture (10–30 cm)	x	(x)	Baumberger et al. (2024)
SOC stocks (0–10 cm)	x	(x)	Haas et al. (2026)
SOC stocks (10–30 cm)	x	(x)	Haas et al. (2026)
C/N ratio (0–10 cm)	x		
pH(H_2O) (0–10 cm)	x		
% WHC (0–10 cm)	x		
Bulk density (0–10 cm)	x		
Slope	(x)	x	DEM from Geobasisdaten: Bayerische Vermessungsverwaltung (2020b)
TWI	(x)	x	DEM from Geobasisdaten: Bayerische Vermessungsverwaltung (2020b)
NDVI	(x)	x	Remote sensing data from Sentinel-2
Vegetation change	(x)	x	Remote sensing data from Sentinel-2
Land use type	(x)	x	Land use from Geobasisdaten: Bayerische Vermessungsverwaltung (2020c) and soil evaluation from Geobasisdaten: Bayerische Vermessungsverwaltung (2020a)

calculated using the slope in radians (S) and the upland contributing area (A; Sørensen et al., 2006):

$$\mathrm{TWI} = \ln\frac{A}{\tan(S)} \quad (2)$$

To obtain spatio-temporal information on vegetation cover (density and vitality of the vegetation), we calculated the Normalised Difference Vegetation Index (NDVI) from the spectral bands of the Sentinel-2 satellite. The Sentinel-2 satellite data have a spatial resolution of 10 m and a temporal resolution of 5 days (ESA, 2015). The NDVI was calculated from the near-infrared (NIR) and red (RED) band (Carlson and Ripley, 1997):

$$\mathrm{NDVI} = \frac{\mathrm{NIR} - \mathrm{RED}}{\mathrm{NIR} + \mathrm{RED}} \quad (3)$$

The technical implementation for calculating the NDVI over the year 2021 and 2022 was carried out in Google Earth Engine (Gorelick et al., 2017). Within this period, all satellite images were compiled and the clouds were masked. The Sentinel-2 scenes were then linearly interpolated in space and time in R (R Core Team, 2024) to create gap-

free time series in daily resolution. In addition, we described the change in vegetation over a period of two weeks, by calculating the difference between the NDVI at the time of the chamber measurement and the NDVI two weeks earlier.

2.4. Effect of landscape heterogeneity on temperature dependence of soil respiration

As temperature is known to be a key predictor of soil respiration (Lloyd and Taylor, 1994), we first investigated the effect of landscape heterogeneity on the temperature dependence of soil respiration. For this purpose, subsets of the previously described data sets were analysed and compared between different levels of heterogeneity. Specifically, our objective was to assess in which extend the variance in the soil respiration – soil temperature relationship could be explained by temperature alone in relation to overall landscape heterogeneity.

We described landscape heterogeneity based on the number of different land use types and the number of different measurement sites. Each data set contained a subset of 60 measurements from different seasons of the year. Data were taken at the following locations for the following purposes:

- **Single forest measurement site**: The data set with low heterogeneity of the landscape contained multiple measurements from a single forest site in the centre of the study area.
- **Multiple forest measurement sites**: To represent a medium heterogeneity of the landscape, we used measurements from different forest sites in the study area.
- **Multiple land use types measurement sites**: The highest heterogeneity of the landscape is represented by measurements from all land use types randomly distributed in the study area.

We modelled the temperature dependency of soil respiration for the three data sets. The relationship between soil respiration (SR) and temperature (T) was described by an exponential function with two fitting parameters (a and b; cf. N. Meyer et al., 2018):

$$SR_T = a \exp(bT) \quad (4)$$

To determine the proportion of explained variance, the coefficient of determination R^2 was calculated. Additionally, the p-value was calculated to evaluate the statistical significance of the exponential relationship between soil respiration and temperature. The Q10 value describes the relative increase in soil respiration with a temperature increase of 10°C and can be determined by the following equation:

$$Q10 = \exp(10b) \quad (5)$$

2.5. Soil respiration modelling and interpretation

To explain and model the relationship between soil respiration and its potential predictors (Table 1), we trained random forest models (Sections 2.5.1 and 2.5.2). The models had two different purposes: Firstly, we aimed at using the model to make spatio-temporal predictions based on all predictors available as raster data (Section 2.5.3). Secondly, our objective was to use the model to analyse the relationship between soil respiration and all potential predictors, including the predictors which were only available as point measurements. A comparison of the models should provide information on whether omitting of soil parameters that were not available as raster data lead to a loss of information in the spatio-temporal modelling. Combining spatial predictions and interpretable machine learning methods, we analysed soil respiration patterns on a landscape scale (Section 2.5.4).

2.5.1. Random forest models

The predictors for soil respiration modelling were selected based on their process-related relevance and their spatial availability to ensure that all predictors have a direct potential explanatory power with respect to soil respiration (Table 1). We created three data sets from the soil respiration measurements and the corresponding predictors and trained three random forest models (Breiman, 2001), (1) to spatio-temporally predict soil respiration, (2) to describe the relationships between soil respiration and all potential predictor variables and (3) to separate the effect of the number of measurements and the number of predictors. The three models were trained with the following data sets:

1. **Model for spatial prediction**: This model included 191 soil respiration measurements combined with the 11 spatially continuously predictors (cf. Table 1; raster data).
2. **Model including all predictors**: This model was based on 116 soil respiration measurements combined with the 15 potentially important predictors (cf. Table 1; point data). It contained the 4 additional predictors % WHC, C/N ratio, bulk density and pH but less training data.
3. **Model for separating effects**: This model included the 116 soil respiration measurements from model 2 combined with the 11 spatially continuously predictors from model 1.

Comparing the three models should reveal whether they learnt similar relationships, how the amount of data affects the prediction performance, and whether omitting soil core data leads to a loss of relevant information.

Technically, the models were built in R (R Core Team, 2024), using the implementation in the ranger package (Wright and Ziegler, 2017) which was accessed via the caret framework (Kuhn, 2008).

2.5.2. Model tuning and validation

For model tuning and validation, we used a nested repeated cross-validation with an external test set. The models were trained based on the training data, tuned using the validation data, and independently evaluated using the test set. For the test set, only data shared across all data sets was used, to ensure the comparability between the models. We first divided these 116 soil respiration measurements and predictors into three folds by temporal stratification, i.e., each fold contained data taken throughout the year. However, for measurement sites with repeated measurements, all data were assigned to the same fold to avoid testing the predictive power of the model for the same spatial locations (cf. H. Meyer et al., 2018). Further soil respiration measurements with associated predictors, which were included in only one of the data sets, were assigned to the training data of the respective model. This data split ensured that the training and test sets never contained the same locations or the same time points. The same procedure was applied to the cross-validation splits. Models were then trained by always leaving one of the three test sets out and tuning the models on the remaining data. For hyperparameter tuning, the respective data were divided into 4 (model with N = 116) or 8 (model with N = 191) spatial folds. This procedure was repeated 10 times to get stable information on the ideal hyperparameter values. The hyperparameters were searched using the root mean squared error (RMSE) as a performance measure. For the number of predictors randomly selected at each split (mtry), we tested all values from 2 to 11 or 15 depending on the number of predictors in the model. For the minimum node size, we tested for values 5, 10, 15, 20 and 25. We trained all models with a fixed number of 100 trees. The coefficient of determination R^2 and the RMSE served as performance measures. To estimate the test error and the cross-validation error, the average performance was calculated over all iterations. The final models for model interpretation and spatial prediction were trained on the basis of the entire data set. The hyperparameters that were selected most frequently during cross-validation were used for these models (mtry = 2 and min node size = 5 for the model including all predictors and the model for separating effects; mtry = 3 and min node size = 5 for the model for spatial prediction).

2.5.3. Model prediction

For the spatio-temporal prediction of soil respiration, the model for spatial prediction (model 1) was applied to the 10 m resolution raster data of all 11 spatial predictors (Fig. 2). Since the predictors soil temperature, soil moisture and SOC stocks were modelled products (cf. Section 2.3.2), the error of the modelled products propagated to the spatial prediction of soil respiration. To estimate the error propagation, we calculated the predictive performance of the trained model on the test set which (1) contained the measured data of soil temperature, soil moisture and SOC stocks and (2) contained the modelled data of soil temperature, soil moisture and SOC stocks. The difference between these calculated errors was used to describe the error propagation.

Predictions were possible with a temporal resolution of one hour following the temporal resolution of soil temperature and soil moisture model. We applied the model to 8 time points per month within the year 2022 selected via temporal stratification and calculated monthly means. We calculated pixel-wise monthly summary statistics (means, minimum, maximum, standard deviation, and range) of soil respiration from the 8 dates per month. For each prediction, we determined the area of applicability (Meyer and Pebesma, 2021) using the implementation from the CAST package (Meyer et al., 2026), which allowed us to exclude model predictions with a high uncertainty due to extrapolation in the predictor space. When averaging spatial predictions of soil respiration, pixels were marked as outside of the area of applicability when ≥50% of the spatial predictions were outside of the area of applicability in the respective pixel.

2.5.4. Interpretation of the model and the spatial predictions

To analyse the relationships learnt by the models, we calculated the partial dependency between soil respiration and each predictor separately. Partial dependency indicates how an individual predictor influences the result of the random forest model while all other predictors are kept constant (Molnar, 2022). Since the spatial patterns of soil respiration result from the specific landscape characteristic, we used Shapley additive explanation to analyse the spatio-temporal influence of all predictor variables. Shapley additive explanation measures the marginal contribution of each predictor to a model prediction. The influence of a variable is calculated by the difference between the predictions with and without this variable, while taking into account all possible orders and combinations of the other variables (Molnar, 2022). We calculated the absolute predictor importance based on Shapley additive explanation, which describes the magnitude of the attribution of each predictor. Furthermore, we investigated the pixel-wise contribution of all 11 predictors. Due to computational costs, we reduced the number of pixels from 4 million to 400,000 by resampling equidistantly. For each predictor, we determined whether the predictor increased or decreased soil respiration for a respective pixel compared to the mean of all predictions. The sum of the positive and negative effects of all predictors led to the final prediction of soil respiration.

3. Results

3.1. Influence of landscape heterogeneity on temperature dependence of soil respiration

The comparison of the temperature dependency of soil respiration in relation to the heterogeneity of the landscape (represented by multiple measurements from one location, measurements from different forest sites, and measurements from a diverse landscape including forests, grasslands, and arable land) showed that soil respiration increased significantly ($p < 0.001$) with increasing temperatures, regardless of the heterogeneity of the landscape (Fig. 3). However, the explainability of soil respiration by soil temperature decreased with increasing heterogeneity of the landscape: Soil respiration taken at a single site could be explained with an R^2 of 0.80. The proportion of explained variance decreased to an R^2 of 0.49 for different forest sites and to an R^2 of 0.22 for the heterogeneous landscape including forests, grasslands and arable land, hence the entire study area of this project.

3.2. Land use effect on soil respiration

Within the study area, the landscape is characterised by the different land use types. Since nearly all soil respiration measurements were taken at different sites, there was a great variability over the course of the year even within each land use type. As expected, higher soil respiration was measured in summer compared to winter in all land use types (Fig. 4). Grassland sites showed higher soil respiration on average (156 mg C m^{-2} h^{-1}) than forests (96 mg C m^{-2} h^{-1}) and arable land (77 mg C m^{-2} h^{-1}). The highest CO_2 effluxes (over 300 mg C m^{-2} h^{-1}) were measured primarily on grassland sites. Soil respiration measurements on grasslands also had the largest variability in summer. Within each land use type, the differences between sites were smallest in winter (Fig. 4).

The predictors used to explain soil respiration (cf. Table 1) were in some cases strongly influenced by land use type (as indicated by distinct value ranges of some predictors within each land use type), which led to dependencies between predictors (Fig. A.1). Forests differed clearly from grasslands and arable land in terms of several soil properties such as C/N ratio, bulk density, and pH (Fig. A.1h, i and j). Forests also exhibited higher SOC stocks than grasslands and arable land in the top 10 cm and at a depths-level from 10 to 30 cm, but also SOC stocks comparable to those of the other land use types (Fig. A.1f and g). Grassland and arable land generally exhibited a very similar range of values for the predictor variables, however, the CO_2 efflux was higher on grassland than on arable land (Fig. A.1). The relationship between vegetation cover, as represented by NDVI, and soil respiration varied clearly between grassland and arable land: High soil respiration often occurred at sites with particularly high NDVI (mainly grassland), and low soil respiration occurred at sites with low NDVI (mainly arable land; Fig. A.1l). Also the temperature sensitivity of soil respiration varied across land use types (Q10 (forest) = 2.6, Q10 (grassland) = 2.2, Q10 (arable land) = 1.6; Fig. A.2).

Particularly in heterogeneous landscapes, a single predictor or even a combination of two predictors is insufficient to adequately describe the variability in soil respiration, suggesting that a combination of all predictors may be necessary for reliable modelling of soil respiration.

3.3. Random forest models for incorporating multiple drivers of soil respiration

Taking all 15 potential predictors in the random forest model into account, soil respiration was modelled with an R^2 of 0.35 and an RMSE of 61 mg C m^{-2} h^{-1}. The evaluation of the model showed that the exclusion of spatially unavailable variables (% WHC, C/N ratio, bulk density and pH) in the model for spatial prediction had no negative effect on the predictability of the model. The model trained with the purpose of spatio-temporal prediction of soil respiration had a model performance of R^2 = 0.39 and RMSE = 61 mg C m^{-2} h^{-1} (Table 2). Since the model was trained with the measurement data of soil temperature, soil moisture and SOC stocks, the error propagation when predicting soil respiration using the modelled soil temperature, soil moisture and SOC stocks had to be considered. Here, a predictive performance of R^2 = 0.37 and RMSE = 63 mg C m^{-2} h^{-1} was calculated, representing the model performance for the spatial predictions.

3.4. Drivers of soil respiration on a landscape scale

The relationships between soil respiration and its predictors learnt in the models can be explored with partial dependency. In both models, similar relationships were learnt (Fig. 5). The soil temperature at a depth of 0–10 cm had the strongest effect on soil respiration indicated by its positive relationship on a wide range of soil respiration values (Fig. 5a) and a high importance based on Shapley additive explanation (Table 3). The models also learnt a positive relationship between soil respiration and soil temperature in a soil depth of 10–30 cm (Fig.

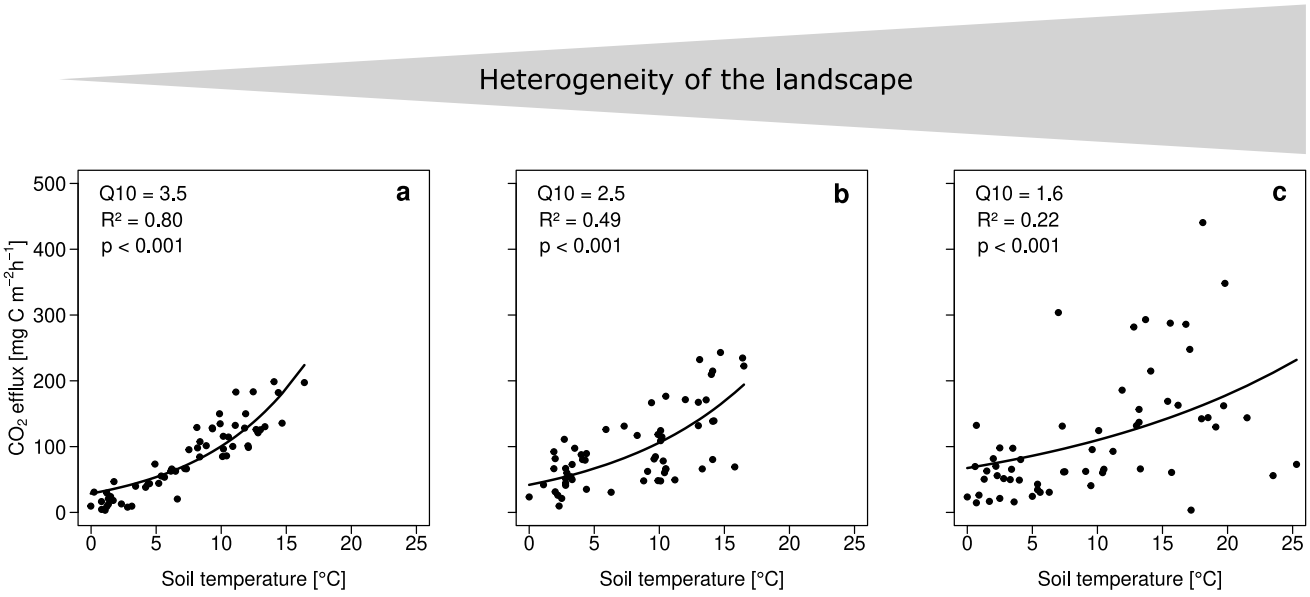

Fig. 3. Dependence of soil respiration on soil temperature for different levels of heterogeneity of the landscape. The heterogeneity is increasing from **a** to **c** and is represented by **a** measurements from a single location in the forest, **b** measurements from different sites in forest area and **c** measurements from grassland, arable land and forest sites. For better comparability, 60 measurements from each of the three datasets were randomly selected. The relationship is modelled by an exponential function. Q10 values represent the relative increase of soil respiration with a 10°C increase in temperature.

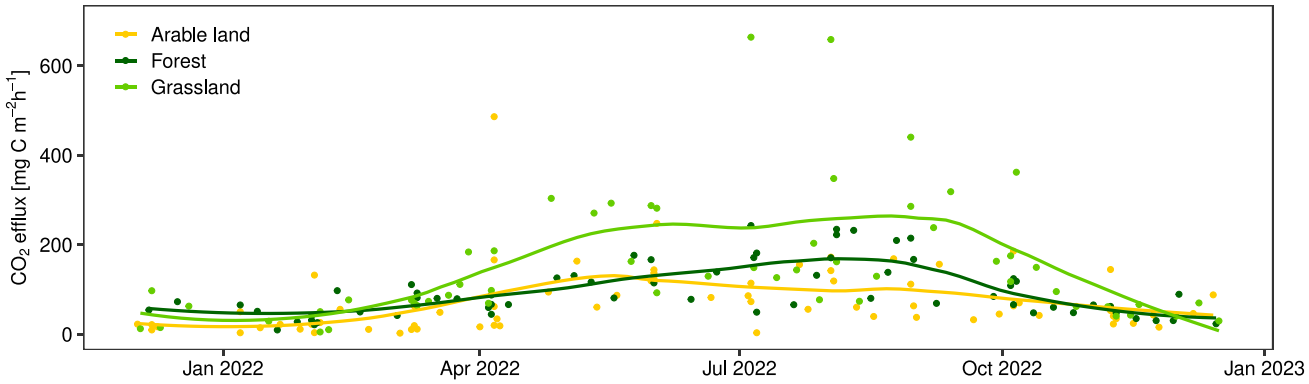

Fig. 4. Temporal course of measured soil respiration at different locations. The colours indicate the land use type. A mean temporal course of the soil respiration per land use type was estimated with locally estimated smoothing.

Table 2
Model performance metrics for different soil respiration model approaches. The columns compare the three model variants where each model is based on different numbers of measurement site and predictors.

Model		(1) Model for spatial prediction		(2) Model including all predictors		(3) Model for separating effects	
	n measurement sites	166		91		91	
	n measurements	191		116		116	
	n predictors	11		15		11	
Error metrics		R^2	RSME	R^2	RSME	R^2	RSME
Cross-validation error		0.44 ± 0.05	80 ± 3	0.36 ± 0.12	58 ± 3	0.37 ± 0.12	57 ± 4
Test error		0.39 ± 0.19	61 ± 9	0.35 ± 0.08	61 ± 5	0.37 ± 0.07	60 ± 4

5b). In both depths, there was a sudden increase in soil respiration at soil temperatures of approximately 10°C (Fig. 5a and b). In addition, NDVI, as a proxy of vegetation density and vitality, had a major influence on soil respiration in the models. Soil respiration increased with increasing NDVI (Fig. 5l). For the change in vegetation, described by the difference in NDVI over a two-week period, both models showed an increase in CO_2 efflux when the vegetation was in a growth phase (Fig. 5m). Soil moisture (measured as volumetric water content) had only a minor effect on soil respiration in the models. A slight increase in soil respiration was observed in response to increased soil moisture in both models and for both soil depths. Particularly high soil moisture at a depth of 10–30 cm led to an increase in soil respiration (Fig. 5c and d). When soil moisture was considered in relation to the maximum water-holding capacity of the sites (which was also determined at the locations where the soil cores were collected), the partial dependency showed a negative relationship (Fig. 5e). Increasing SOC stocks by up to 60 t/ha in the upper 10 cm of the soil led to higher soil respiration predictions (Fig. 5f). SOC stocks in 10–30 cm soil depth showed minor

Table 3
SHAP feature importance for the predictor variables in the model for spatial prediction and in the model including all predictors. The SHAP feature importance describes the magnitude of the attribution of each predictor (Molnar, 2022). Explanation of abbreviations: SOC = soil organic carbon, % WHC = percent of water holding capacity, TWI = topographic wetness index, NDVI = Normalised Difference Vegetation Index.

Predictor	Importance in model for spatial prediction	Importance in model including all predictors
Soil temperature (0–10 cm)	37.8	11.4
Soil temperature (10–30 cm)	17.0	10.7
Soil moisture (0–10 cm)	3.96	1.02
Soil moisture (10–30 cm)	2.80	3.16
SOC stocks (0–10 cm)	8.51	5.35
SOC stocks (10–30 cm)	1.67	3.10
C/N ratio (0–10 cm)	x	1.29
pH(H_2O) (0–10 cm)	x	1.06
% WHC (0–10 cm)	x	9.77
Bulk density (0–10 cm)	x	5.91
Land use type	2.04	4.07
Slope	2.65	0.97
TWI	3.27	1.73
NDVI	4.69	1.56
Vegetation change	3.90	2.36

effects on soil respiration (Fig. 5g). The topography was described by the TWI and the slope. Focussing on the range of predictor values supported by many measurements, a positive relationship between soil respiration and TWI occurred (Fig. 5n). Higher soil respiration was expected for low slopes (which typically occur in valleys; Fig. 5o). Similarly as in the measurement data, both models indicate that on grasslands, the CO_2 efflux tended to be higher on average, while on arable land the CO_2 efflux tended to be lower on average (Figs. A.1k and 5k). The C/N ratio, bulk density, pH and % WHC, were only used in the model including all potential predictors of soil respiration. The pH showed no effect on soil respiration and very low C/N ratio had a slightly positive effect on soil respiration. For lower bulk density, slightly higher soil respiration could be expected (Fig. 5h, i and j). However, these soil properties were highly dependent on the land use type (Fig. A.1e, h, i and j).

3.5. Spatio-temporal patterns of soil respiration

In our spatio-temporal model predictions (Fig. 6), the monthly mean soil respiration exhibited an annual cycle with a lower CO_2 efflux in the winter months and a higher CO_2 efflux in the summer months. Spatial variations were especially pronounced in summer, whereas in the winter months, only minimal spatial variations were recognisable. At all times of the year, a homogeneous soil respiration pattern emerged along the mountain ridge, which stretches diagonally from south-west to north-east. The remaining areas of the study site were characterised by heterogeneous patches with variations in soil respiration. In June, predictions in some areas were excluded due to high uncertainty, leading to the smallest area of applicability compared to the other months. In general, only a few predictions were outside the area of applicability (Fig. 6).

The highest mean soil respiration of 177 mg C m^{-2} h^{-1} was predicted in June. The maximum soil respiration of 496 mg C m^{-2} h^{-1} was predicted on one day in August. Within one month and across the entire study area, soil respiration exhibited strong spatial and temporal variations. The largest spatial variations (i.e., the difference in soil respiration in the study area at one single time point) were predicted in June, with a range of 415 mg C m^{-2} h^{-1}. Also during winter spatial variations occurred, e.g., in December, spatial variations of 130 mg C m^{-2} h^{-1} were still predicted (Table 4).

3.6. Explanation of spatio-temporal soil respiration patterns

To study the spatial patterns of soil respiration, we analysed the predictions for three exemplary dates in more detail. The prediction from January 15th, 12 pm was characterised by a homogeneous low soil respiration, the prediction from May 15th, 12 pm showed pronounced spatial differences and the prediction from September 15th, 12 pm showed a high but spatially homogeneous soil respiration (Figs. 7 and 8). Using Shapley additive explanation, we determined the pixel-wise contribution of all predictors to the respective prediction of soil respiration. For the three selected dates, all predictors had an influence on the spatial patterns of soil respiration, whereas the strength of the influence differed. The positive or negative contribution of the predictors to soil respiration was evaluated relative to the mean predicted soil respiration of 106.5 mg C m^{-2} h^{-1}.

Soil temperature had a strong influence on soil respiration over the entire study area. Spatio-temporal patterns were similar in 0–10 cm and 10–30 cm soil depth. In January, the soil temperature at both depths was very homogeneous with spatial temperature differences of approximately 3°C. The low temperatures between 0°C and 3°C had a negative influence on soil respiration throughout the study area. In May, soil temperature, similar to soil respiration, had strong spatial variations. At a soil depth of 0–10 cm, the temperature varied between 7°C and 19°C and at a soil depth of 10–30 cm, the soil temperature varied between 7°C and 15°C. High soil temperatures had a positive influence on soil respiration, while the lower temperatures had a negative influence. Here, the spatial patterns of soil respiration strongly followed the patterns of soil temperature. In September, the soil temperature in 0–10 cm soil depth varied between 12°C and 17°C (12°C and 18°C in 10–30 cm soil depth). Nevertheless, the positive effect on soil respiration was very homogeneous and spatial patterns of the contribution of soil temperature to soil respiration were weakly pronounced.

Furthermore, NDVI had a strong effect on the spatial patterns of soil respiration. While the NDVI in the forest areas (the main part of the coniferous forest extends diagonally from south-west to north-east) was rather low and constant throughout the year, there were strong fine-scale variations in the areas with mixed land use in May and September. These fine-scale variations also led to fine-scale variations in the contribution of NDVI to soil respiration predictions. Generally, low NDVI had a negative effect on soil respiration and high NDVI had a positive effect on soil respiration. Furthermore, there was a particularly strong increase in NDVI in May. This vegetation growth also had a positive effect on soil respiration (Fig. 7).

In addition to the temporally dynamic predictors, we also analysed the influence of predictors that were assumed to be constant throughout the year 2022 (Fig. 8). The spatial patterns of predicted soil respiration were driven by the spatial distribution of SOC stocks at 0–10 cm soil depth. High SOC stocks increased soil respiration, while low SOC stocks decreased it. Topography had a strong fine-scale effect on the spatial patterns of soil respiration. Areas with a low slope and high TWI (valleys) enhanced soil respiration. The valleys were predominantly covered by grasslands, which had a positive effect on soil respiration. Forest and arable land generally had a negative effect on soil respiration.

4. Discussion

4.1. Soil respiration modelling at a landscape scale

We have shown that soil respiration on the plot scale was explained up to 80% by soil temperature, while on the landscape scale only 22% of the variability in soil respiration was explained by soil temperature (Fig. 3). Thus, for the modelling of soil respiration on the landscape scale, a variety of predictors was necessary to account for the spatio-temporal patterns. The inclusion of these spatio-temporal predictors

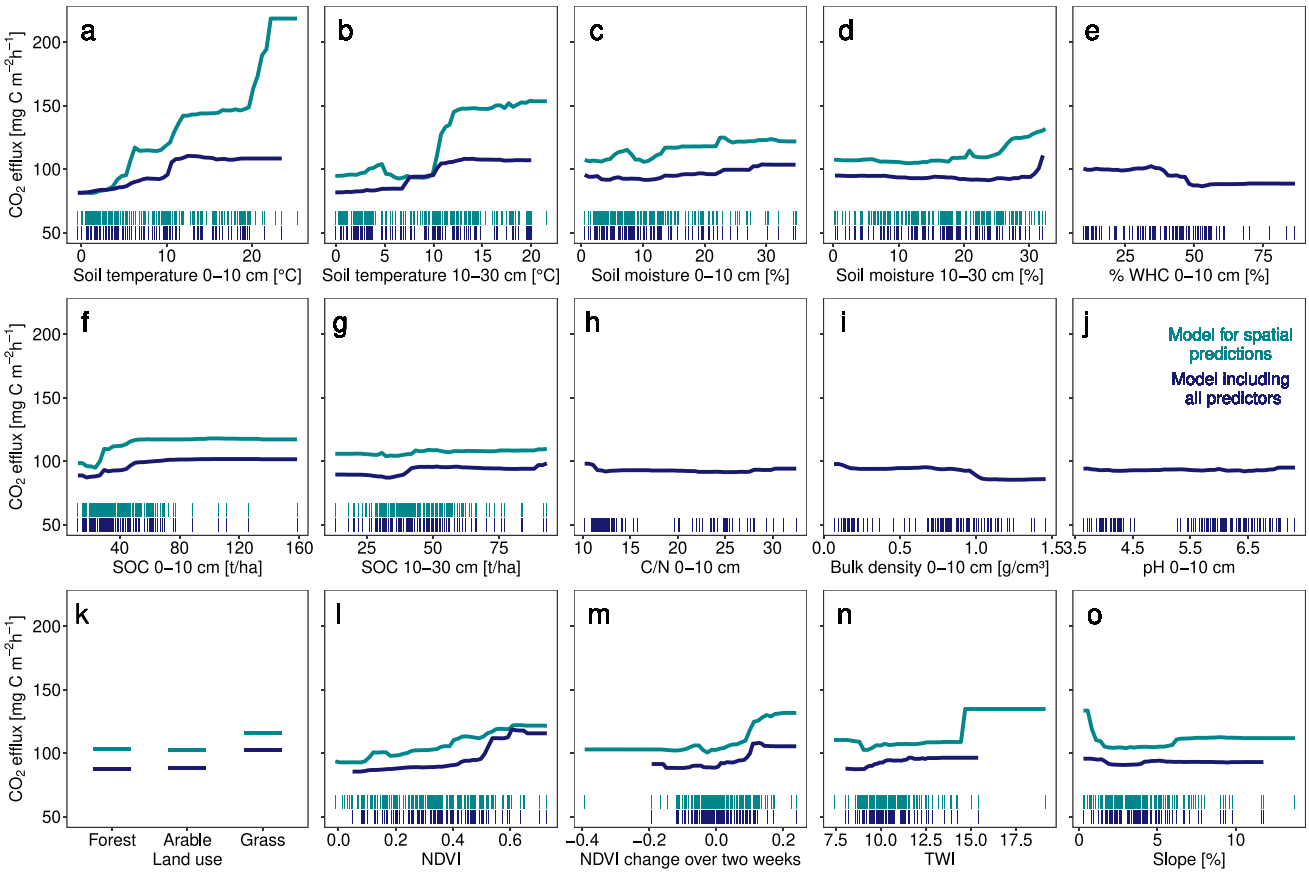

Fig. 5. Partial dependency between soil respiration and all predictor variables in the models. The dark blue colour indicates the results of the model including all predictors which is based on 116 measurements and 15 predictors while the turquoise colour indicates the results of the model for spatial predictions which is based on 192 measurements and 11 predictors. The rug marks indicate the distribution of the predictor variables. In forests, data of the organic layer is presented instead of data from the 0–10 cm mineral soil depth and the lower topsoil is considered to extend from 0–30 cm, replacing the standard 10–30 cm soil depth.

Table 4
Spatio-temporal summary statistics of predicted monthly soil respiration in mg C m^{-2} h^{-1}, including mean, standard deviation, minimum, maximum and range. The range describes the maximum range at a single point in time within a month.

	Jan	Feb	Mar	Apr	May	Jun	Jul	Aug	Sep	Oct	Nov	Dec
Mean	55	55	64	85	144	177	166	170	146	116	82	56
Standard deviation	17	18	16	20	45	51	36	40	34	27	16	16
Minimum	11	10	11	14	51	66	76	82	38	47	15	11
Maximum	200	181	182	238	353	487	480	496	373	332	198	144
Range	164	162	150	185	288	415	388	405	285	247	161	130

allowed for the explanation of 39% of the variability in soil respiration in a heterogeneous landscape (Table 2). This corresponds to an RMSE of 61 mg C m^{-2} h^{-1}, which, given the data splitting strategy, also reflects the performance of the model in predicting soil respiration at unknown time points and unknown locations. Numerous factors could have a negative influence on the model performance. However, the small area outside the area of applicability in the model predictions indicates that the measurements in the study area were conducted at representative locations (Fig. 6). Increasing the number of measurement points from 116 to 191 while using the same set of predictor variables only led to a minimal improvement of the model, suggesting that a sufficient number of measurements had already been used for model training (Table 2). Although we included many relevant predictors, additional drivers may still have been required to improve model performance: In particular, important drivers such as microbial community composition and microbial biomass, which can only be assessed through extensive laboratory analysis, were not included in this study. Furthermore, comprehensive spatial information on agricultural management, such as tillage and fertilisation, was not available (Luo and Zhou, 2006). Among others these drivers could be important for explaining the spatio-temporal patterns of soil respiration at the landscape scale. For future work, the investigation of means to obtain data on these drivers or appropriate proxies in high spatial and temporal resolution is a promising way forward.

Soil temperature, SOC stocks, and vegetation cover turned out to be strong predictors, explaining a substantial portion of the variability in soil respiration (Table 3). Land use type, topography and soil moisture also influenced the spatial patterns of soil respiration, although they had a weaker influence (Table 3 and Figs. 5, 7 and 8). Further site-specific soil properties, such as the C/N ratio and pH, showed only

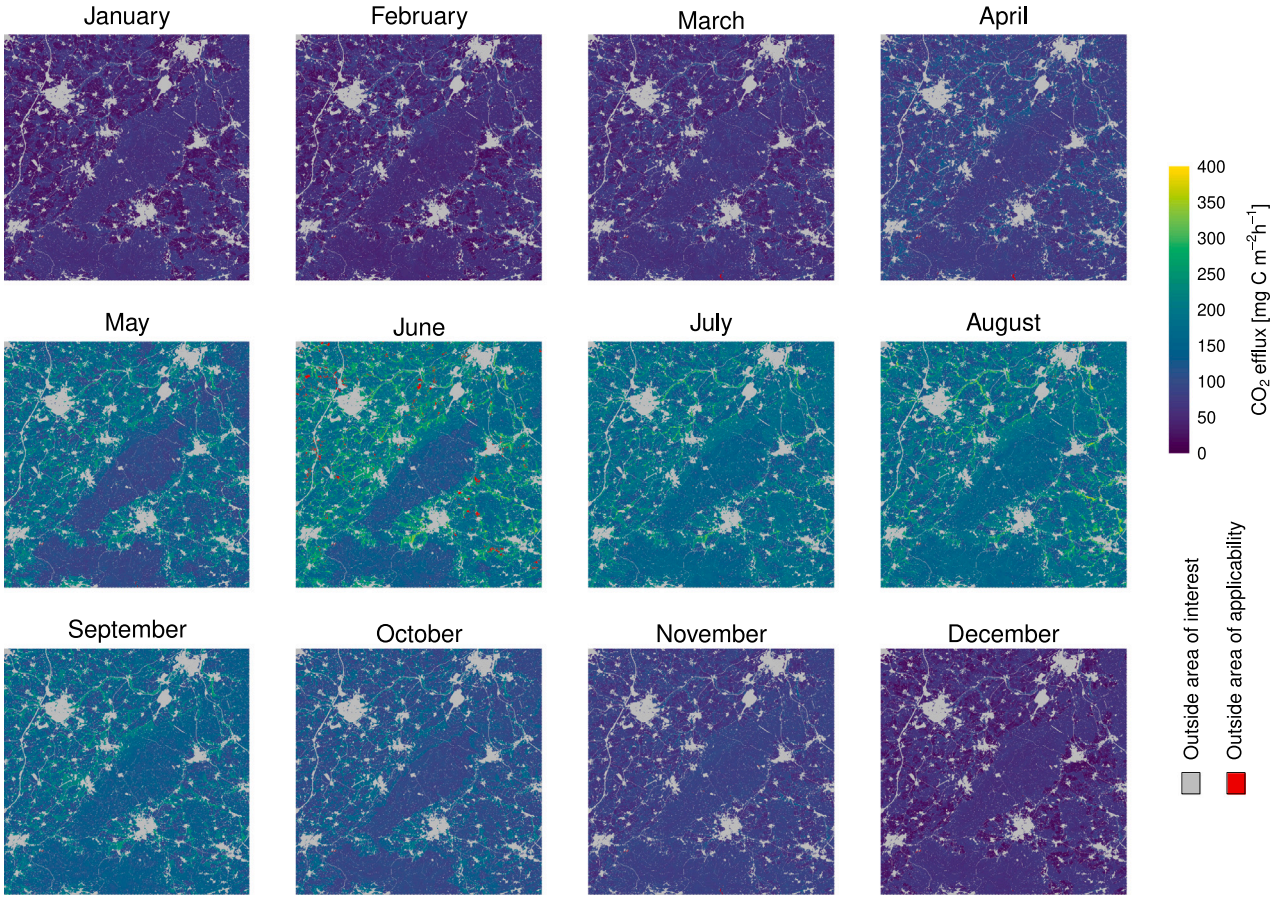

Fig. 6. Monthly mean soil respiration for the study area with a size of 20 km × 20 km. A stratified sample of 8 spatial predictions each month was averaged. Grey areas indicate areas out of interest. Red areas are outside the area of applicability.

minor effects on soil respiration (Fig. 5). Since the four predictors C/N ratio, pH, bulk density, and % WHC were not spatially available, they were not included in the model for spatial predictions of soil respiration. However, these four predictors differed considerably between the three land use types (Fig. A.1). Thus, the predictor land use type implicitly contained these information in the model for spatial predictions, which needed to be considered when interpreting the results. However, the exclusion of these predictors from the spatial prediction model did not negatively affect the performance of this model (Table 2). Accordingly, the set of spatially available predictors (cf. Table 1) proved suitable for modelling soil respiration on the landscape scale.

For the spatially continuous prediction of soil respiration, spatially continuous data of the explanatory variables were necessary. Although not all predictors are generally available in high resolution, our previous studies (Baumberger et al., 2024; Haas et al., 2026) have enabled us to ensure that soil temperature, soil moisture and SOC stocks were available in the appropriate resolution for our study area. The resolution of the spatial model prediction of the target variables depends on the spatial resolution of the predictor variables (Fritsch et al., 2020). As all predictors that potentially drive spatial variations of soil respiration were available with a spatial resolution of 10 m (Table 1), we also modelled soil respiration with a spatial resolution of 10 m. Soil temperature and soil moisture were modelled with a resolution of 1 h to capture diurnal changes (Baumberger et al., 2024), which enabled us to temporally model soil respiration also with a resolution of 1 h. Overall, 10 m in space and 1 h in time was an adequate resolution, since we showed short-term temporal variations and fine-scale spatial variations of soil respiration (Fig. 6). This has enabled us to model soil respiration on the landscape scale in a resolution that, to our knowledge, has rarely been achieved.

Since the model predictions of soil temperature, soil moisture, and SOC stocks were associated with uncertainties (cf. Section 2.3.2), the uncertainties of these predictors were propagated into the soil respiration predictions. An assessment of this error propagation showed that the R^2 decreased by only 0.02 due to the model errors of the predictors soil temperature, soil moisture, and SOC stocks. This minor propagation error can be attributed to the very high predictive accuracy of the soil temperature model, which was the most important predictor of soil respiration, while soil moisture, which showed comparatively high uncertainty, was a less relevant predictor for soil respiration.

In this study, our goal was not only to make spatial predictions using machine learning but also to interpret these predictions to deepen our understanding of spatio-temporal soil respiration dynamics and their drivers on a landscape scale. However, it must be taken into account that the relations learnt by the model were not necessarily ecologically causal, since the models were optimised to find patterns that best predict the target variable rather than to identify causal relationships. Hence, even a high model performance is not a guarantee for process-based correctness of relationships between soil respiration and its predictors (Murdoch et al., 2019). Wadoux et al. (2020) have shown that spatial patterns of a target variable can also be explained by unrelated predictors, which can lead to misinterpretation. To avoid this and to improve ecological interpretability, we have included only predictor variables in the model that are known to potentially have an influence from an ecological perspective. The relationships between

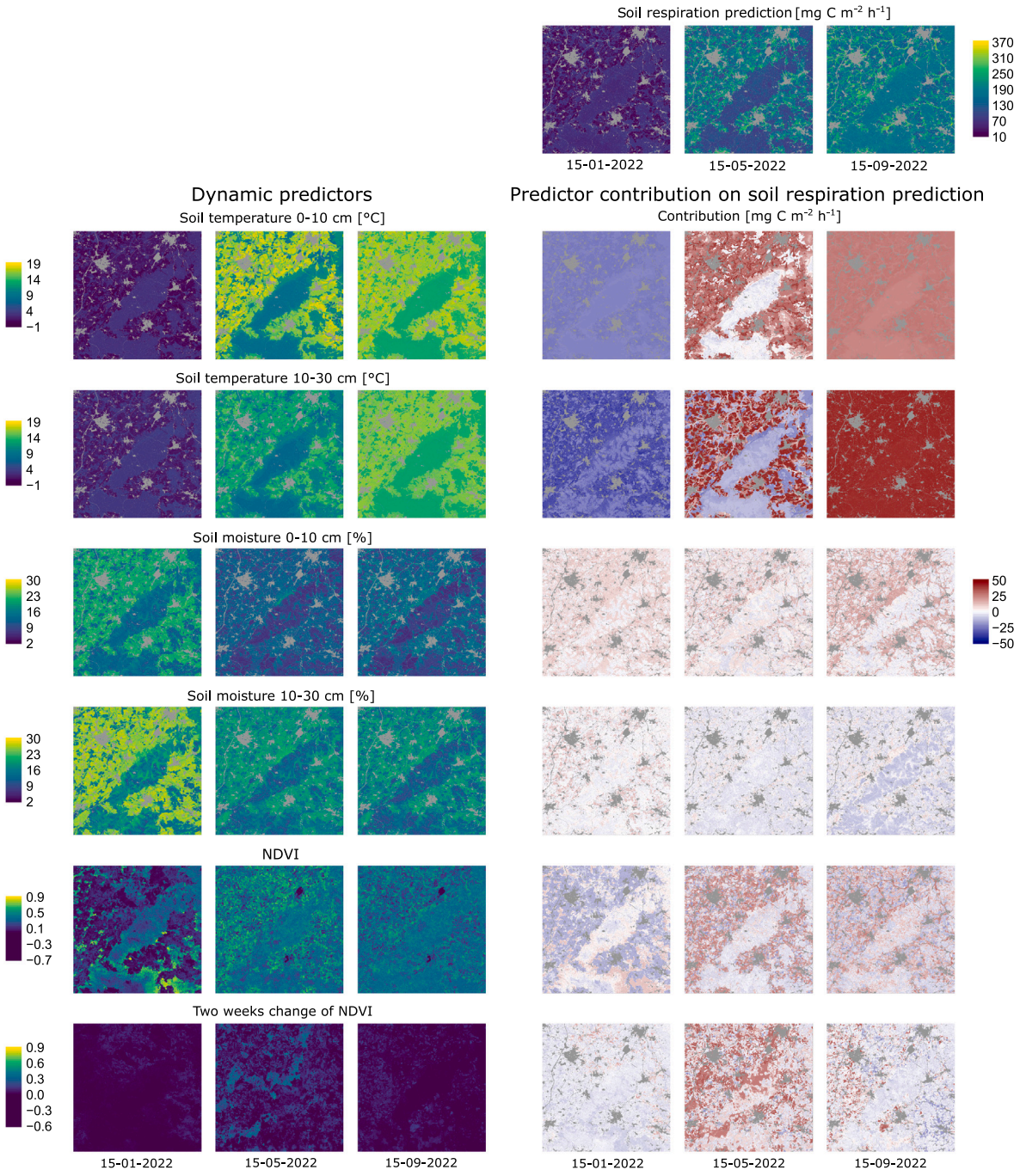

Fig. 7. Explanation of three different spatial predictions of soil respiration based on the dynamic predictor variables. Predictions were made for the 15th of January, 15th of May and 15th of September, each at 12 pm and are shown in the top row. The three columns on the left show the dynamic predictor variables for the respective points in time. Alongside, in the three right columns, the predictor contribution based on Shapley additive explanation is shown for the respective points in time. The positive (reddish) or negative (bluish) effect refers to a mean value of 106.5 mg C m^{-2} h^{-1} (the mean prediction). This figure needs to be considered in combination with Fig. 8.

soil respiration and its predictors cannot be derived from the machine learning model alone, and interpretation in combination with expert knowledge was required. Using partial dependency, we verified the relationships learnt in the models, which will be discussed in Section 4.2. To explain the patterns of soil respiration within the exemplary landscape, Shapley additive explanation was applied, allowing the identification of specific spatial patterns which will be further discussed in Section 4.3.

4.2. Influence of predictors on soil respiration

It is well known that soil respiration is strongly influenced by soil temperature (Lloyd and Taylor, 1994). However, we have seen that this effect decreased with increasing heterogeneity of the landscape (Fig. 3) and that further predictors were important in predicting the amount of CO_2 efflux on a landscape scale (Fig. 5). Hibbard et al. (2005) have also concluded that soil respiration of individual sites is well explained

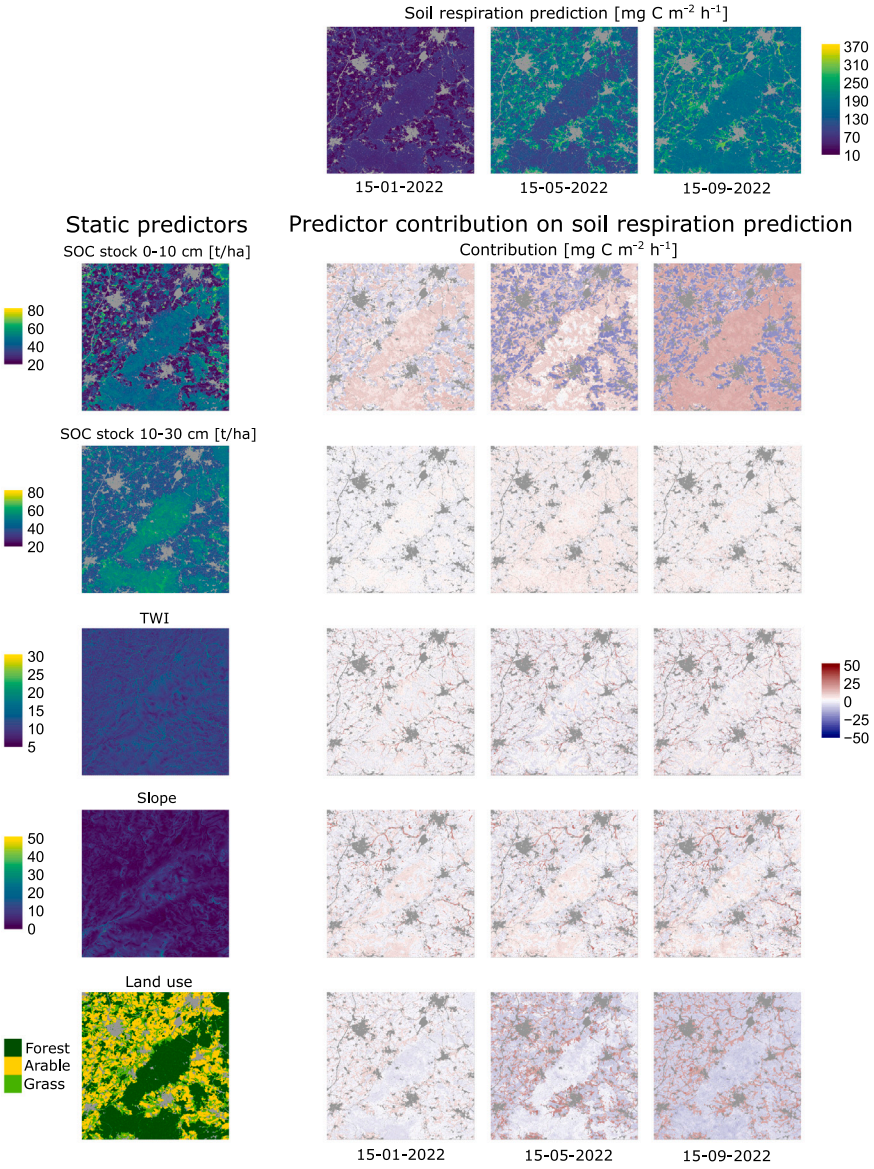

Fig. 8. Explanation of three different spatial predictions of soil respiration based on the static predictor variables. Predictions were made for the 15th of January, 15th of May and 15th of September, each at 12 pm and are shown in the top row. The column on the left shows the static predictor variables. Alongside, in the three right columns, the predictor contribution based on Shapley additive explanation is shown for the respective points in time. The positive (reddish) or negative (bluish) effect refers to a mean value of 106.5 mg C m^{-2} h^{-1} (the mean prediction). This figure needs to be considered in combination with Fig. 7.

by soil temperature and soil moisture, but to explain soil respiration of multiple sites, information on soil properties and vegetation cover increases in relevance. However, we have shown that soil temperature remained the most important driver of spatio-temporal patterns of soil respiration even in a heterogeneous landscape (Table 3, Figs. 5 and 7).

Since our study was based on field measurements and not on controlled laboratory measurements, it is important to consider that changes in soil temperature were often accompanied by simultaneous changes in soil moisture, making it challenging to isolate the effects of both drivers individually. On the other hand, studying soil respiration under real-world conditions allowed accounting for the natural interactions and variability of environmental drivers. The year 2022 in Germany was characterised by a particularly dry summer (DWD, 2023). Therefore, in the data set, warm conditions were generally associated with drought, while cold conditions were associated with higher soil moisture. The frequent combination of cold and moist conditions was probably also one of the reasons why we did not observe a strong effect of soil moisture on soil respiration (Fig. 5c–e). The optimal combination of soil moisture and soil temperature conditions for microbes, for which we expected the highest soil respiration, rarely occurred. Our models indicated only slight variations of soil respiration due to soil moisture. When considering soil moisture as volumetric soil water content, we observed a slightly positive relationship with soil respiration (Fig. 5c and d). However, when relating soil water content to the water-holding capacity (%WHC) of a site, it became evident that soils tending towards water saturation reduced soil respiration (Fig. 5e). Usually, soil moisture had been demonstrated to have a small effect on soil respiration in a range where soils are neither very dry nor wet and only influences soil respiration when either water or oxygen limitation occurs (Moyano et al., 2012). Assessments of the effects of soil moisture on soil respiration also vary in the literature. For instance, Fang and Moncrieff (2001) have reported no significant differences in soil respiration under varying soil moisture conditions and further studies reported controversial effects of soil moisture on soil respiration (Cook and Orchard, 2008; Dörr and Münnich, 1987; Luan et al., 2013).

SOC stocks were the third most important predictor for the spatial predictions of soil respiration after soil temperature in the different

depth intervals, and SOC stocks were also an important predictor in the model that included all predictors (Table 3). In both models, a positive relationship with soil respiration was observed. This indicates that greater SOC stocks are also associated with greater carbon availability, providing more substrate that can be decomposed by microorganisms, thus leading to higher soil respiration rates. However, SOC stocks were strongly influenced by land use, with the highest stocks found in forest areas (Fig. A.1). Here, the litter had a much wider C/N ratio, compared to grasslands and arable lands (Fig. A.1h). Coniferous leaf litter decomposes slowly, accumulating in thick organic layers and transforming more slowly into stable SOC stocks than litter with a narrower C/N ratio (Klein-Raufhake et al., 2025; Prescott, 2010). In Bavarian coniferous forests, Wiesmeier et al. (2013) showed that the organic layer contains up to 35% of the total SOC.

In this study, the models predicted on average highest soil respiration for grasslands, lower soil respiration for forests, and lowest soil respiration for arable land (Fig. 5k). However, forest sites had the highest availability of easily degradable organic matter for decomposition processes indicated by high SOC stocks (Fig. A.1f) and a high Q10 value (Fig. A.2). Nevertheless, the soil respiration on grasslands was higher than on forest sites. The reason for this was likely that the trees in forests buffered the solar radiation and therefore the soil temperature reached a lower maximum in forests than on grasslands (Baumberger et al., 2024), indicating the strong temperature dependency of soil respiration. On arable land, the lowest soil respiration was predicted, even though they reached the highest temperatures. The low SOC stocks (Fig. A.1f) and low Q10 value (Fig. A.2) indicated the lowest substrate availability for decomposition processes on arable land. The reason for this is frequent tillage and low return of organic residues, which is also associated with low contents of soil microorganisms and thus lower microbial activity (Poeplau et al., 2020). Thus, a combination of high soil respiration potential given by the availability of organic material and root biomass as well as high temperature, as on grasslands, is required for high soil respiration.

Vegetation cover, described by the NDVI, showed a prominent effect in the models. The partial dependency showed a positive relationship between the NDVI and soil respiration (Fig. 5l), which indicated that soil respiration increased with increasing vegetation density. Reichstein et al. (2003) and Hibbard et al. (2005) have also shown that the vegetation density is positively related to soil respiration. Although dense vegetation can lower soil temperatures, which may reduce temperature-dependent microbial activity (Fig. 5a), plants still exert an overall positive effect on soil respiration. In our study, vegetation-rich grassland sites with high soil respiration were clearly distinguishable from the vegetation-sparse arable sites with low soil respiration (Fig. A.1l). Vegetation density is also reflected in the root biomass. A major component of soil respiration (up to 90%) is root respiration (Hanson et al., 2000). As a result of regular ploughing, plants on arable land are annual and have less opportunity to develop roots resulting in reduced root respiration which is a possible reason for the lower soil respiration on arable land. In addition, the increase in vegetation also had an influence on soil respiration, whereby a strong increase in vegetation was accompanied by high soil respiration (Fig. 5m). This effect was also found in Bahn et al. (2008), who reported a relationship between temporal changes in vegetation density and soil respiration. Especially during the growth phase, plants release more root exudates (Přikryl and Vančura, 1980). These root exudates can easily be metabolised by microorganisms that promote the CO_2 efflux from soils (Kuzyakov and Larionova, 2006). This effect may explain the generally high soil respiration in grassland, especially from April onwards (Figs. 4 and 6). Hou et al. (2025) have shown increasing soil respiration rates due to root exudates after drought periods. This probably explains the extremely high soil respiration measurements and predictions on grasslands in summer (Figs. 4 and 6).

Another factor, which could have an effect on soil respiration of grasslands but also arable land, is fertilisation. Although there are no spatial data on timing and types of fertilisation that could be used in this study, we described the nutrient content in soil by the C/N ratio, which is also influenced by fertilisation. The partial dependency indicated just a slightly positive effect of a low C/N ratio (indicating high nutrient availability) on soil respiration (Fig. 5h). However, the effects of nitrogen fertilisation on soil respiration are also very variable, since e.g. Craine et al. (2001) showed a positive effect and e.g. Kowalenko et al. (1978) showed a negative effect on soil respiration. The nutrient availability influences many processes in the soil that can either inhibit or promote soil respiration (Luo and Zhou, 2006).

This highlights the complexity of the drivers of soil respiration and further explains why soil respiration is challenging to predict on a landscape scale. Nevertheless, we have shown that the models have learnt meaningful relationships based on the training data.

4.3. Spatio-temporal patterns of soil respiration

The modelling approach of this study enabled, to the knowledge of the authors, the first predictions of spatial patterns of soil respiration across a heterogeneous landscape in such a high spatio-temporal resolution. From our model predictions, we could infer the large variations occurring both spatially in a 20 km × 20 km section of a central European landscape and temporally over the course of a year (Fig. 6 and Table 4). The spatio-temporal patterns of soil respiration were shaped by the patterns of their drivers (Figs. 7 and 8). Applying the interpretable machine learning method Shapley additive explanation to the raster data of the predictors, we analysed the contribution of all predictors in detail. Thus, we could go beyond analysing relationships between response and predictor variables and were able to comprehensively analyse the influence of each predictor on soil respiration for each location in our study area under given environmental conditions. This enabled us to investigate the influence of the specific landscape characteristics on spatio-temporal soil respiration patterns.

The predicted spatio-temporal patterns of soil respiration on the landscape scale were connected to the specific patterns of its environmental predictors. Overall, soil temperature patterns had the strongest influence on spatio-temporal soil respiration patterns (Table 3). The temporal patterns of soil respiration strongly follow the temporal dynamics of soil temperature, resulting in pronounced diurnal and annual variations. Especially during the summer months, fluctuations in soil temperature of up to 10°C over the course of a day frequently occurred at the non-forested sites in the study area (Baumberger et al., 2024). An increase of 10°C could increase soil respiration by approximately 50 mg C m^{-2} h^{-1}, depending on the temperature range (Fig. 5a). Throughout the year, the modelled soil respiration varied between 10 mg C m^{-2} h^{-1} and 496 mg C m^{-2} h^{-1} (Table 4). These temporal variations were explained not only by soil temperature, but also by soil moisture, vegetation density, and vegetation change. The largest spatial variations in soil respiration driven by soil temperature occurred when soil temperature also had the greatest variations (Fig. 7). Strong temperature variations in a landscape usually occur in the summer months (Baumberger et al., 2024). The spatial distribution of forested areas within the landscape became especially apparent due to their characteristic lower temperatures and associated reduced soil respiration (Fig. 7). Spatial soil temperature patterns in a landscape were influenced by the land use type and topography (Baumberger et al., 2024). Land use type and topography patterns were therefore passed through soil temperature to soil respiration. Thus multiple landscape-specific information were already contained in the soil temperature. These findings are in line with research by Arevalo et al. (2010), who have also shown that site specific soil temperature differences mainly explained the spatial differences in soil respiration. The spatial patterns of SOC stocks in 0–10 cm soil depth mainly followed the patterns of land use (Haas et al., 2026). Here again, the spatial distribution of forested areas was particularly prominent, with a generally higher SOC stock in the top 10 cm compared to arable land and grasslands,

which have a positive influence on soil respiration. This implies that a substantial portion of soil respiration in the forests was promoted by the high SOC stocks. Nevertheless, the effect of temperature overlaid the effect of SOC stocks, as in forest areas with low temperature and high SOC, low soil respiration still occurred (Fig. 7). Within a land use type, vegetation cover and vegetation change (described by the NDVI and the NDVI change over two weeks) revealed further variations that had a major influence on the spatial pattern of soil respiration. Within a single field or grassland, the NDVI was generally consistent but it differed between neighbouring units of the same land use. As a result, the spatial patterns of soil respiration reflected the shapes of the agricultural units. Thus, vegetation cover could differentiate the spatial patterns of soil respiration within land use types. Soil respiration within a unit of grassland or arable area was relatively homogeneous (Fig. 6) and did not have a strong influence on the spatial patterns of soil respiration on the landscape scale. Crum et al. (2016) have shown that intensive management leads to a decrease in the spatial variability of soil respiration. These findings align with the intensively managed arable land and grasslands in the Fichtelgebirge mountains. In the valleys, areas with increased soil respiration could be observed (Fig. 6). There are multiple potential reasons for the positive effect of valleys. These sites were likely moister, as indicated by the high TWI and their proximity to streams. In addition, there are more grassland sites in the valleys, which exhibit high soil respiration due to their vegetation and soil properties (as discussed in Section 4.2).

From this it follows that spatial patterns in soil respiration in a heterogeneous landscape were mainly induced by land use, vegetation cover, and topography. These landscape characteristics also drove spatial patterns of the other predictors such as soil temperature, soil moisture, and SOC stocks (Baumberger et al., 2024; Haas et al., 2026), which thereby also transmit the spatial patterns of land use, vegetation cover, and topography to soil respiration. The predictor land use type reflected multiple factors that influence soil respiration, e.g., soil properties such as pH, C/N ratio, and bulk density, which differ strongly between the land use types (Fig. A.1). The multitude of drivers influencing soil respiration resulted in strong spatio-temporal variability of soil respiration in a landscape (Table 4). During the summer months, several high-respiration patches developed, which were located on grasslands in depressions. These areas exhibited higher soil moisture due to their proximity to the streams (Figs. 7 and 8). Overall, these grasslands were characterised by vital vegetation, high root density, and substantial production of root exudates (as discussed in Section 4.2), and also provided optimal temperature and moisture conditions for microbial activity and root respiration. This highlights the importance of soil moisture for soil respiration, even though soil moisture played a comparatively minor role in the model for spatio-temporal predictions of soil respiration.

The detection of very fine spatial patterns indicated the presence of fine-scale heterogeneity (Fig. 6), highlighting the need for high-resolution data in predictive modelling. Especially individual land use types and management units needed to be differentiated, which was possible with the resolution of 10 m that was used in this study. The temporal variation in soil respiration was mainly induced by the temporal variation of soil temperature, which is characterised by an annual cycle that includes strong daily variations in the study area (Baumberger et al., 2025). Thus, sub-daily temporal resolution was required to capture fine-scale temporal variation in soil respiration. Our findings underline the substantial heterogeneity of soil respiration across a heterogeneous landscape and emphasise the influence of soil temperature and thus also land use and topography. The pronounced variation within land use types highlights the importance of fine-scale drivers, such as vegetation cover and its changes, that are often overlooked in large-scale models. These insights can inform future upscaling efforts and contribute to more accurate predictions of carbon fluxes in heterogeneous landscapes under changing environmental conditions.

5. Conclusion

With 191 CO_2 efflux measurements from 166 different sites, we created a comprehensive data set to investigate spatio-temporal patterns of soil respiration on a landscape scale. By combining these measurements with a variety of potential environmental drivers in a random forest model, we developed a model to predict soil respiration with a resolution of 10 m in space and 1 h in time for our 20 km × 20 km study area in the Fichtelgebirge mountains in Germany. Model predictions revealed large spatio-temporal variability of soil respiration on the landscape scale, highlighting the importance of modelling soil respiration in high resolution. We have shown that spatio-temporal patterns of soil respiration were explained by a variety of drivers with complex interactions. Interpretable machine learning allowed disentangling the effects of multiple interacting environmental factors on soil respiration. The consideration of soil respiration under real-world conditions, including the explanation of the individual contributions of all predictors, provided insights on spatio-temporal soil respiration patterns on the landscape scale. In addition, to gaining insights into soil respiration on a landscape scale, methodological progress was made by developing a modelling approach for predicting high-resolution soil respiration and demonstrating the value of interpretable machine learning techniques for the analysis of model predictions.

CRediT authorship contribution statement

Maiken Baumberger: Writing – original draft, Visualization, Software, Project administration, Methodology, Investigation, Formal analysis, Data curation, Conceptualization. **Bettina Haas:** Writing – review & editing, Investigation, Data curation. **Werner Borken:** Writing – review & editing, Investigation. **Jakub Nowosad:** Writing – review & editing, Methodology. **Laura Giese:** Writing – review & editing, Methodology. **Theresa Klein-Raufhake:** Writing – review & editing. **Ute Hamer:** Writing – review & editing. **Nele Meyer:** Writing – review & editing, Supervision, Funding acquisition, Conceptualization. **Hanna Meyer:** Writing – review & editing, Supervision, Funding acquisition, Conceptualization.

Funding

The research was conducted in the project Carbon4D, funded by the German Research Foundation (DFG; Project number 455085607). Further supported was provided by the project Reversal (BiodivRestore ERA-NET Cofund; DFG Project number 491288730). Jakub Nowosad has received the financial support of the European Union's Horizon Europe research and innovation programme under the Marie Skłodowska-Curie grant agreement No. 101147446.

Declaration of competing interest

The authors declare that they have no known competing financial interests or personal relationships that could have appeared to influence the work reported in this paper.

Appendix

See Figs. A.1 and A.2.

Data availability

Data, scripts and models are available on GitHub: https://github.com/MaikenBaumberger/SR.

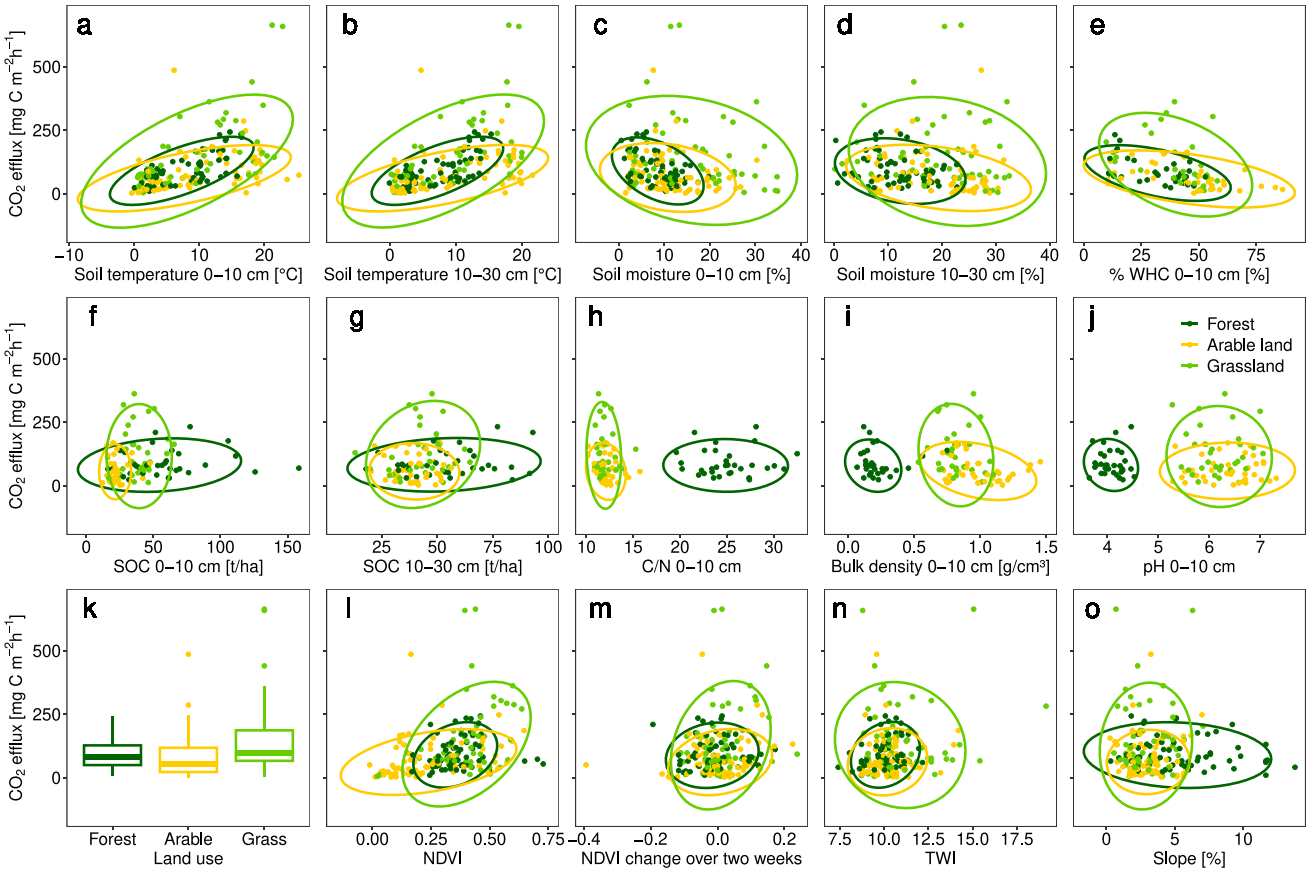

Fig. A.1. Relationships between soil respiration and its predictors, separated by land use type. For each land use type, the spread of the relationship between soil respiration and the predictor variable is visualised by a Gaussian ellipse. The ellipses show the 95% confidence level of the respective distribution. Note that the panels e–j contain only 116 data points from the 91 locations where soil cores were taken while the remaining panels contain 191 measurements. In forests, data of the organic layer is presented instead of data from the 0–10 cm mineral soil depth and the lower topsoil is considered to extend from 0–30 cm, replacing the standard 10–30 cm soil depth.

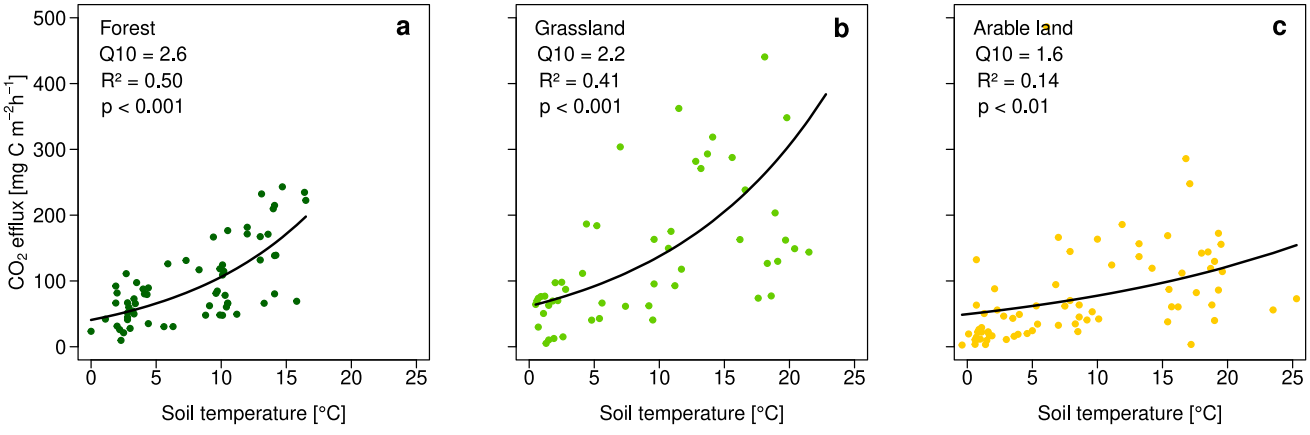

Fig. A.2. Dependence of soil respiration on soil temperature for each land use type separately, where **a** shows forest (N = 64), **b** shows grassland (N = 53) and **c** shows arable land (N = 74). The relationship is modelled by an exponential function. Q10 values represent the rate at which soil respiration change with a 10°C increase in temperature.

References

Arevalo, C.B.M., Bhatti, J.S., Chang, S.X., Jassal, R.S., Sidders, D., 2010. Soil respiration in four different land use systems in north central Alberta, Canada. J. Geophys. Res. 115 (G1), 2009JG001006. http://dx.doi.org/10.1029/2009JG001006.

Bahn, M., Rodeghiero, M., Anderson-Dunn, M., Dore, S., Gimeno, C., Drösler, M., Williams, M., Ammann, C., Berninger, F., Flechard, C., Jones, S., Balzarolo, M., Kumar, S., Newesely, C., Priwitzer, T., Raschi, A., Siegwolf, R., Susiluoto, S., Tenhunen, J., Wohlfahrt, G., Cernusca, A., 2008. Soil respiration in European grasslands in relation to climate and assimilate supply. Ecosystems 11 (8), 1352–1367. http://dx.doi.org/10.1007/s10021-008-9198-0.

Bardgett, R.D., Mommer, L., De Vries, F.T., 2014. Going underground: Root traits as drivers of ecosystem processes. Trends Ecol. Evol. 29 (12), 692–699. http://dx.doi.org/10.1016/j.tree.2014.10.006.

Baumberger, M., Haas, B., Sivakumar, S., Ludwig, M., Meyer, N., Meyer, H., 2024. High-resolution soil temperature and soil moisture patterns in space, depth and time: An interpretable machine learning modelling approach. Geoderma 451, 117049. http://dx.doi.org/10.1016/j.geoderma.2024.117049.

Baumberger, M., Haas, B., Tewes, W., Risse, B., Meyer, N., Meyer, H., 2025. Gated recurrent units for modelling time series of soil temperature and moisture: An assessment of performance and process reflectivity. Env. Model. Softw. 183, 106245. http://dx.doi.org/10.1016/j.envsoft.2024.106245.

Bayerische Vermessungsverwaltung, 2020a. Geobasisdaten: BoSch (Bodenschätzung), München.

Bayerische Vermessungsverwaltung, 2020b. Geobasisdaten: DGM10 (digitales geländemodel 10m), München.

Bayerische Vermessungsverwaltung, 2020c. Geobasisdaten: Tatsächliche nutzung objektbereich vegetation, München.

Bayerisches Landesamt für Umwelt, 2020. ÜBK25 (Digitale übersichtsbodenkarte von bayern im maßstab 1:25000, Augsburg.

Bond-Lamberty, B., Bailey, V.L., Chen, M., Gough, C.M., Vargas, R., 2018. Globally rising soil heterotrophic respiration over recent decades. Nature 560 (7716), 80–83. http://dx.doi.org/10.1038/s41586-018-0358-x.

Borchard, N., Schirrmann, M., Hebel, C.V., Schmidt, M., Baatz, R., Firbank, L., Vereecken, H., Herbst, M., 2015. Spatio-temporal drivers of soil and ecosystem carbon fluxes at field scale in an upland grassland in Germany. Agric. Ecosyst. Env. 211, 84–93. http://dx.doi.org/10.1016/j.agee.2015.05.008.

Borken, W., Matzner, E., 2009. Reappraisal of drying and wetting effects on C and N mineralization and fluxes in soils. Glob. Chang. Biol. 15 (4), 808–824. http://dx.doi.org/10.1111/j.1365-2486.2008.01681.x.

Borken, W., Xu, Y.-J., Davidson, E.A., Beese, F., 2002. Site and temporal variation of soil respiration in European beech, Norway spruce, and Scots pine forests. Glob. Chang. Biol. 8 (12), 1205–1216. http://dx.doi.org/10.1046/j.1365-2486.2002.00547.x.

Breiman, L., 2001. Random forests. Mach. Learn. 45 (1), 5–32. http://dx.doi.org/10.1023/A:1010933404324.

Carlson, T.N., Ripley, D.A., 1997. On the relation between NDVI, fractional vegetation cover, and leaf area index. Remote Sens. Environ. 62 (3), 241–252. http://dx.doi.org/10.1016/S0034-4257(97)00104-1.

Chatterjee, A., Jenerette, G., 2011. Changes in soil respiration Q10 during drying–Rewetting along a semi-arid elevation gradient. Geoderma 163 (3–4), 171–177. http://dx.doi.org/10.1016/j.geoderma.2011.04.003.

Cleveland, C.C., Nemergut, D.R., Schmidt, S.K., Townsend, A.R., 2007. Increases in soil respiration following labile carbon additions linked to rapid shifts in soil microbial community composition. Biogeochemistry 82 (3), 229–240. http://dx.doi.org/10.1007/s10533-006-9065-z.

Cook, F.J., Orchard, V.A., 2008. Relationships between soil respiration and soil moisture. Soil Biol. Biochem. 40 (5), 1013–1018. http://dx.doi.org/10.1016/j.soilbio.2007.12.012.

Craine, J.M., Wedin, D.A., Reich, P.B., 2001. Grassland species effects on soil CO_2 flux track the effects of elevated CO_2 and Nitrogen. New Phytol. 150 (2), 425–434. http://dx.doi.org/10.1046/j.1469-8137.2001.00103.x.

Crowther, T.W., Todd-Brown, K.E.O., Rowe, C.W., Wieder, W.R., Carey, J.C., Machmuller, M.B., Snoek, B.L., Fang, S., Zhou, G., Allison, S.D., Blair, J.M., Bridgham, S.D., Burton, A.J., Carrillo, Y., Reich, P.B., Clark, J.S., Classen, A.T., Dijkstra, F.A., Elberling, B., Emmett, B.A., Estiarte, M., Frey, S.D., Guo, J., Harte, J., Jiang, L., Johnson, B.R., Kröel-Dulay, G., Larsen, K.S., Laudon, H., Lavallee, J.M., Luo, Y., Lupascu, M., Ma, L.N., Marhan, S., Michelsen, A., Mohan, J., Niu, S., Pendall, E., Peñuelas, J., Pfeifer-Meister, L., Poll, C., Reinsch, S., Reynolds, L.L., Schmidt, I.K., Sistla, S., Sokol, N.W., Templer, P.H., Treseder, K.K., Welker, J.M., Bradford, M.A., 2016. Quantifying global soil carbon losses in response to warming. Nature 540 (7631), 104–108. http://dx.doi.org/10.1038/nature20150.

Crum, S.M., Liang, L.L., Jenerette, G.D., 2016. Landscape position influences soil respiration variability and sensitivity to physiological drivers in mixed-use lands of Southern California, USA. JGR Biogeosciences 121 (10), 2530–2543. http://dx.doi.org/10.1002/2016JG003469.

Curiel Yuste, J., Baldocchi, D.D., Gershenson, A., Goldstein, A., Misson, L., Wong, S., 2007. Microbial soil respiration and its dependency on carbon inputs, soil temperature and moisture. Glob. Chang. Biol. 13 (9), 2018–2035. http://dx.doi.org/10.1111/j.1365-2486.2007.01415.x.

Dörr, H., Münnich, K.O., 1987. Annual variation in soil respiration in selected areas of the temperate zone. Tellus B 39 (1–2), 114. http://dx.doi.org/10.3402/tellusb.v39i1-2.15329.

DWD, 2023. Klimastatusbericht Deutschland Jahr 2022. Technical Report, Deutscher Wetterdienst, Geschäftsbereich Klima und Umwelt, Offenbach.

ESA, 2015. Sentinel-2 user handbook.

Euskirchen, E.S., Chen, J., Gustafson, E.J., Ma, S., 2003. Soil respiration at dominant patch types within a managed northern Wisconsin landscape. Ecosystems 6 (6), 595–607. http://dx.doi.org/10.1007/PL00021505.

Fang, C., Moncrieff, J., 2001. The dependence of soil CO2 efflux on temperature. Soil Biol. Biochem. 33 (2), 155–165. http://dx.doi.org/10.1016/S0038-0717(00)00125-5.

Foken, T. (Ed.), 2017. Energy and Matter Fluxes of a Spruce Forest Ecosystem. In: Ecological Studies, vol. 229, Springer International Publishing, Cham, http://dx.doi.org/10.1007/978-3-319-49389-3.

Friedman, J.H., 2001. Greedy function approximation: A gradient boosting machine. Ann. Statist. 29 (5), http://dx.doi.org/10.1214/aos/1013203451.

Fritsch, M., Lischke, H., Meyer, K.M., 2020. Scaling methods in ecological modelling. Methods Ecol. Evol. 11 (11), 1368–1378. http://dx.doi.org/10.1111/2041-210X.13466.

Gasch, C.K., Hengl, T., Gräler, B., Meyer, H., Magney, T.S., Brown, D.J., 2015. Spatio-temporal interpolation of soil water, temperature, and electrical conductivity in 3D + T: The Cook Agronomy Farm data set. Spat. Stat. 14, 70–90. http://dx.doi.org/10.1016/j.spasta.2015.04.001.

Gorelick, N., Hancher, M., Dixon, M., Ilyushchenko, S., Thau, D., Moore, R., 2017. Google earth engine: Planetary-scale geospatial analysis for everyone. Remote Sens. Environ. 202, 18–27. http://dx.doi.org/10.1016/j.rse.2017.06.031.

Haas, B., Baumberger, M., Müller, M., Schweers, J., Hülsmann, L., Lehndorff, E., Meyer, H., Meyer, N., 2026. Regional spatial and vertical patterns of SOC stocks in a low mountain landscape in Germany. Geoderma Reg. e01102. http://dx.doi.org/10.1016/j.geodrs.2026.e01102.

Hanson, P.J., Edwards, N.T., Garten, C.T., Andrews, J.A., 2000. Separating root and soil microbial contributions to soil respiration: A review of methods and observations. Biogeochemistry 48, 115–146. http://dx.doi.org/10.1023/A:1006244819642.

Hibbard, K.A., Law, B.E., Reichstein, M., Sulzman, J., 2005. An analysis of soil respiration across northern hemisphere temperate ecosystems. Biogeochemistry 73 (1), 29–70. http://dx.doi.org/10.1007/s10533-004-2946-0.

Hirano, T., 2005. Seasonal and diurnal variations in topsoil and subsoil respiration under snowpack in a temperate deciduous forest. Glob. Biogeochem. Cycles 19 (2), 2004GB002259. http://dx.doi.org/10.1029/2004GB002259.

Hou, F., Hinojosa, L., Enderle, E., Jansen, B., Morriën, E., De Vries, F.T., 2025. Root exudates from drought-affected plants increase soil respiration across a range of grassland species. Soil Biol. Biochem. 203, 109731. http://dx.doi.org/10.1016/j.soilbio.2025.109731.

Jiang, S., Sweet, L.-b., Blougouras, G., Brenning, A., Li, W., Reichstein, M., Denzler, J., Shangguan, W., Yu, G., Huang, F., Zscheischler, J., 2024. How interpretable machine learning can benefit process understanding in the geosciences. Earth's Futur. 12 (7), e2024EF004540. http://dx.doi.org/10.1029/2024EF004540.

Klein-Raufhake, T., Hölzel, N., Schaper, J.J., Elmer, M., Fornfeist, M., Linnemann, B., Meyer, M., Neuenkamp, L., Rentemeister, K., Santora, L., Wöllecke, J., Hamer, U., 2025. Disentangling the impact of forest management intensity components on soil biological processes. Glob. Chang. Biol. 31 (1), e70018. http://dx.doi.org/10.1111/gcb.70018.

Kowalenko, C., Ivarson, K., Cameron, D., 1978. Effect of moisture content, temperature and nitrogen fertilization on carbon dioxide evolution from field soils. Soil Biol. Biochem. 10 (5), 417–423. http://dx.doi.org/10.1016/0038-0717(78)90068-8.

Kuhn, M., 2008. Building predictive models in r using the caret package. Stat. Sof. 28 (5), http://dx.doi.org/10.18637/jss.v028.i05.

Kuzyakov, Ya.V., Larionova, A.A., 2006. Contribution of rhizomicrobial and root respiration to the CO2 emission from soil (A review). Eurasian Soil Sci. 39 (7), 753–764. http://dx.doi.org/10.1134/S106422930607009X.

Lary, D.J., Alavi, A.H., Gandomi, A.H., Walker, A.L., 2016. Machine learning in geosciences and remote sensing. Geosci. Front. 7 (1), 3–10. http://dx.doi.org/10.1016/j.gsf.2015.07.003.

Liu, S., Plaza, C., Ochoa-Hueso, R., Trivedi, C., Wang, J., Trivedi, P., Zhou, G., Piñeiro, J., Martins, C.S.C., Singh, B.K., Delgado-Baquerizo, M., 2023. Litter and soil biodiversity jointly drive ecosystem functions. Glob. Chang. Biol. 29 (22), 6276–6285. http://dx.doi.org/10.1111/gcb.16913.

Lloyd, J., Taylor, J.A., 1994. On the temperature dependence of soil respiration. Funct. Ecol. 8 (3), 315. http://dx.doi.org/10.2307/2389824, arXiv:2389824.

Luan, J., Liu, S., Wang, J., Zhu, X., 2013. Factors affecting spatial variation of annual apparent Q10 of soil respiration in two warm temperate forests. PLoS One 8 (5), e64167. http://dx.doi.org/10.1371/journal.pone.0064167.

Lundberg, S.M., Lee, S.-I., 2017. A unified approach to interpreting model predictions. In: Guyon, I., Luxburg, U.V., Bengio, S., Wallach, H., Fergus, R., Vishwanathan, S., Garnett, R. (Eds.), Advances in Neural Information Processing Systems. vol. 30, Curran Associates, Inc.

Luo, Y., Zhou, X., 2006. Soil Respiration and the Environment. Elsevier Academic Press, Amsterdam; Boston.

Martin, J.G., Bolstad, P.V., 2009. Variation of soil respiration at three spatial scales: Components within measurements, intra-site variation and patterns on the landscape. Soil Biol. Biochem. 41 (3), 530–543. http://dx.doi.org/10.1016/j.soilbio.2008.12.012.

Meyer, H., Ludwig, M., Milà, C., Linnenbrink, J., Schumacher, F., 2026. The CAST package for training and assessment of spatial prediction models. In: Rocchini, D. (Ed.), R Coding for Ecology. In: Use R! Springer Nature Switzerland, Cham, pp. 247–266. http://dx.doi.org/10.1007/978-3-031-99665-8_11, URL https://link.springer.com/10.1007/978-3-031-99665-8_11.

Meyer, N., Meyer, H., Welp, G., Amelung, W., 2018. Soil respiration and its temperature sensitivity (Q10): Rapid acquisition using mid-infrared spectroscopy. Geoderma 323, 31–40. http://dx.doi.org/10.1016/j.geoderma.2018.02.031.

Meyer, H., Pebesma, E., 2021. Predicting into unknown space? Estimating the area of applicability of spatial prediction models. Methods Ecol. Evol. 12 (9), 1620–1633. http://dx.doi.org/10.1111/2041-210X.13650.

Meyer, H., Reudenbach, C., Hengl, T., Katurji, M., Nauss, T., 2018. Improving performance of spatio-temporal machine learning models using forward feature selection and target-oriented validation. Env. Model. Softw. 101, 1–9. http://dx.doi.org/10.1016/j.envsoft.2017.12.001.

Meyer, N., Welp, G., Amelung, W., 2018a. The temperature sensitivity (Q10) of soil respiration: Controlling factors and spatial prediction at regional scale based on environmental soil classes. Glob. Biogeochem. Cycles 32 (2), 306–323. http://dx.doi.org/10.1002/2017GB005644.

Meyer, N., Welp, G., Rodionov, A., Borchard, N., Martius, C., Amelung, W., 2018b. Nitrogen and phosphorus supply controls soil organic carbon mineralization in tropical topsoil and subsoil. Soil Biol. Biochem. 119, 152–161. http://dx.doi.org/10.1016/j.soilbio.2018.01.024.

Molnar, C., 2022. Interpretable Machine Learning: A Guide for Making Black Box Models Explainable, second ed. Christoph Molnar, Munich, Germany.

Moyano, F.E., Vasilyeva, N., Bouckaert, L., Cook, F., Craine, J., Curiel Yuste, J., Don, A., Epron, D., Formanek, P., Franzluebbers, A., Ilstedt, U., Kätterer, T., Orchard, V., Reichstein, M., Rey, A., Ruamps, L., Subke, J.-A., Thomsen, I.K., Chenu, C., 2012. The moisture response of soil heterotrophic respiration: Interaction with soil properties. Biogeosciences 9 (3), 1173–1182. http://dx.doi.org/10.5194/bg-9-1173-2012.

Muhr, J., Borken, W., 2009. Delayed recovery of soil respiration after wetting of dry soil further reduces C losses from a Norway spruce forest soil. J. Geophys. Res. 114 (G4), 2009JG000998. http://dx.doi.org/10.1029/2009JG000998.

Muhr, J., Borken, W., Matzner, E., 2009. Effects of soil frost on soil respiration and its radiocarbon signature in a Norway spruce forest soil. Glob. Chang. Biol. 15 (4), 782–793. http://dx.doi.org/10.1111/j.1365-2486.2008.01695.x.

Murdoch, W.J., Singh, C., Kumbier, K., Abbasi-Asl, R., Yu, B., 2019. Definitions, methods, and applications in interpretable machine learning. Proc. Natl. Acad. Sci. USA 116 (44), 22071–22080. http://dx.doi.org/10.1073/pnas.1900654116.

Poeplau, C., Jacobs, A., Don, A., Vos, C., Schneider, F., Wittnebel, M., Tiemeyer, B., Heidkamp, A., Prietz, R., Flessa, H., 2020. Stocks of organic carbon in German agricultural soils—Key results of the first comprehensive inventory. J. Plant Nutr. Soil Sci. 183 (6), 665–681. http://dx.doi.org/10.1002/jpln.202000113.

Prescott, C.E., 2010. Litter decomposition: What controls it and how can we alter it to sequester more carbon in forest soils? Biogeochemistry 101 (1–3), 133–149. http://dx.doi.org/10.1007/s10533-010-9439-0.

Přikryl, Z., Vančura, V., 1980. Root exudates of plants: VI. Wheat root exudation as dependent on growth, concentration gradient of exudates and the presence of bacteria. Plant Soil 57 (1), 69–83. http://dx.doi.org/10.1007/BF02139643.

Prolingheuer, N., Scharnagl, B., Graf, A., Vereecken, H., Herbst, M., 2014. On the spatial variation of soil rhizospheric and heterotrophic respiration in a winter wheat stand. Agric. For. Meteorol. 195–196, 24–31. http://dx.doi.org/10.1016/j.agrformet.2014.04.016.

R Core Team, 2024. R: A Language and Environment for Statistical Computing. R Foundation for Statistical Computing. R Core Team, Vienna, Austria.

Raich, J.W., Tufekcioglu, A., 2000. Vegetation and soil respiration: Correlations and controls. Biogeochemistry 48, 71–90. http://dx.doi.org/10.1023/A:1006112000616.

Reichstein, M., Beer, C., 2008. Soil respiration across scales: The importance of a model–data integration framework for data interpretation. J. Plant Nutr. Soil Sci. 171 (3), 344–354. http://dx.doi.org/10.1002/jpln.200700075.

Reichstein, M., Rey, A., Freibauer, A., Tenhunen, J., Valentini, R., Banza, J., Casals, P., Cheng, Y., Grünzweig, J.M., Irvine, J., Joffre, R., Law, B.E., Loustau, D., Miglietta, F., Oechel, W., Ourcival, J.-M., Pereira, J.S., Peressotti, A., Ponti, F., Qi, Y., Rambal, S., Rayment, M., Romanya, J., Rossi, F., Tedeschi, V., Tirone, G., Xu, M., Yakir, D., 2003. Modeling temporal and large-scale spatial variability of soil respiration from soil water availability, temperature and vegetation productivity indices. Glob. Biogeochem. Cycles 17 (4), 2003GB002035. http://dx.doi.org/10.1029/2003GB002035.

Richardson, J., Chatterjee, A., Darrel Jenerette, G., 2012. Optimum temperatures for soil respiration along a semi-arid elevation gradient in southern California. Soil Biol. Biochem. 46, 89–95. http://dx.doi.org/10.1016/j.soilbio.2011.11.008.

Schindlbacher, A., Schnecker, J., Takriti, M., Borken, W., Wanek, W., 2015. Microbial physiology and soil CO_2 efflux after 9 years of soil warming in a temperate forest – No indications for thermal adaptations. Glob. Chang. Biol. 21 (11), 4265–4277. http://dx.doi.org/10.1111/gcb.12996.

Schulze, K., Borken, W., Muhr, J., Matzner, E., 2009. Stock, turnover time and accumulation of organic matter in bulk and density fractions of a Podzol soil. Eur. J. Soil Sci. 60 (4), 567–577. http://dx.doi.org/10.1111/j.1365-2389.2009.01134.x.

Shi, B., Jin, G., 2016. Variability of soil respiration at different spatial scales in temperate forests. Biol. Fertil. Soils 52 (4), 561–571. http://dx.doi.org/10.1007/s00374-016-1100-1.

Shibistova, O., Lloyd, J., Evgrafova, S., Savushkina, N., Zrazhevskaya, G., Arneth, A., Knohl, A., Kolle, O., Schulze, E.-D., 2002. Seasonal and spatial variability in soil CO2 efflux rates for a central Siberian Pinus sylvestris forest. Tellus B 54 (5), 552–567. http://dx.doi.org/10.1034/j.1600-0889.2002.01348.x.

Six, J., Conant, R.T., Paul, E.A., Paustian, K., 2002. Stabilization mechanisms of soil organic matter: Implications for C-saturation of soils. Plant Soil 241, 155–176. http://dx.doi.org/10.1023/A:1016125726789.

Sørensen, R., Zinko, U., Seibert, J., 2006. On the calculation of the topographic wetness index: Evaluation of different methods based on field observations. Hydrol. Earth Syst. Sci. 10 (1), 101–112. http://dx.doi.org/10.5194/hess-10-101-2006.

Subke, J.-A., Reichstein, M., Tenhunen, J.D., 2003. Explaining temporal variation in soil CO2 efflux in a mature spruce forest in Southern Germany. Soil Biol. Biochem. 35 (11), 1467–1483. http://dx.doi.org/10.1016/S0038-0717(03)00241-4.

Tang, J., Baldocchi, D.D., 2005. Spatial–temporal variation in soil respiration in an oak–grass savanna ecosystem in California and its partitioning into autotrophic and heterotrophic components. Biogeochemistry 73 (1), 183–207. http://dx.doi.org/10.1007/s10533-004-5889-6.

Turner, M.G., 1989. Landscape ecology: The effect of pattern on process. Annu. Rev. Ecol. Syst. 20, 171–197. http://dx.doi.org/10.1146/annurev.es.20.110189.001131.

Von Lützow, M., Kögel-Knabner, I., Ludwig, B., Matzner, E., Flessa, H., Ekschmitt, K., Guggenberger, G., Marschner, B., Kalbitz, K., 2008. Stabilization mechanisms of organic matter in four temperate soils: Development and application of a conceptual model. J. Plant Nutr. Soil Sci. 171 (1), 111–124. http://dx.doi.org/10.1002/jpln.200700047.

Wadoux, A.M.J.-C., Saby, N.P.A., Martin, M.P., 2023. Shapley values reveal the drivers of soil organic carbon stock prediction. Soil 9 (1), 21–38. http://dx.doi.org/10.5194/soil-9-21-2023.

Wadoux, A.M.J.-C., Samuel-Rosa, A., Poggio, L., Mulder, V.L., 2020. A note on knowledge discovery and machine learning in digital soil mapping. Eur. J. Soil Sci. 71 (2), 133–136. http://dx.doi.org/10.1111/ejss.12909.

Wiesmeier, M., Prietzel, J., Barthold, F., Spörlein, P., Geuß, U., Hangen, E., Reischl, A., Schilling, B., Von Lützow, M., Kögel-Knabner, I., 2013. Storage and drivers of organic carbon in forest soils of southeast Germany (Bavaria) – Implications for carbon sequestration. For. Ecol. Manag. 295, 162–172. http://dx.doi.org/10.1016/j.foreco.2013.01.025.

Wright, M.N., Ziegler, A., 2017. Ranger : A fast implementation of random forests for high dimensional data in *C++* and *R*. J. Stat. Soft. 77 (1), 1–17. http://dx.doi.org/10.18637/jss.v077.i01.